MPMI Vol. X, No. X, XXXX, pp. X-X, https://doi.org/10.1094/MPMI-03-22-0063-R

Rhizomania: Hide and Seek of *Polymyxa betae* and the Beet Necrotic Yellow Vein Virus with *Beta vulgaris*

Alain Decroës,[1] Mathieu Mahillon,[2] Margaux Genard,[1] Charlotte Lienard,[1] Gipsi Lima-Mendez,[3] David Gilmer,[4] Claude Bragard,[1] and Anne Legrève[1,†]

[1] Phytopathology-Applied Microbiology, Earth and Life Institute, UCLouvain, Louvain-la-Neuve, 1348, Belgium
[2] Plant Protection Department, Agroscope, Nyon, 1260, Switzerland
[3] Louvain Institute of Biomolecular Science and Technology, UCLouvain, Louvain-la-Neuve, 1348, Belgium
[4] Institut de biologie moléculaire des plantes, CNRS UPR2357, Université de Strasbourg, Strasbourg, 67084, France

Accepted for publication 8 July 2022.

The molecular interactions between *Polymyxa betae*, the protist vector of sugar beet viruses, beet necrotic yellow vein virus (BNYVV), the causal agent of rhizomania, and *Beta vulgaris* have not been extensively studied. Here, the transmission of BNYVV to sugar beet by *P. betae* zoospores was optimized using genetically characterized organisms. Molecular interactions of aviruliferous and viruliferous protist infection on sugar beet were highlighted by transcriptomic analysis. *P. betae* alone induced limited gene expression changes in sugar beet, as a biotrophic asymptomatic parasite. Most differentially expressed plant genes were down-regulated and included resistance gene analogs and cell wall peroxidases. Several enzymes involved in stress regulation, such as the glutathione-*S*-transferases, were significantly induced. With BNYVV, the first stages of the *P. betae* life cycle on sugar beet were accelerated with a faster increase of relative protist DNA level and an earlier appearance of sporangia and sporosori in plants roots. A clear activation of plant defenses and the modulation of genes involved in plant cell wall metabolism were observed. The *P. betae* transcriptome in the presence of BNYVV revealed induction of genes possibly involved in the switch to the survival stage. The interactions were different depending on the presence or absence of the virus. *P. betae* alone alleviates plant defense response, playing hide-and-seek with sugar beet and allowing for their mutual development. Conversely, BNYVV manipulates plant defense and promotes the rapid invasion of plant roots by *P. betae*. This accelerated colonization is accompanied by the development of thick-walled resting spores, supporting the virus survival.

Keywords: *Beet necrotic yellow vein virus*, *Plasmodiophorida*, *Polymyxa betae*, Rhizaria, RNA-seq, sugar beet, virus vector

[†]Corresponding author: A. Legrève; anne.legreve@uclouvain.be

Funding: This work was funded by Université Catholique de Louvain. Computational resources were partially provided by the Consortium des Équipements de Calcul Intensif, funded by the Fonds de la Recherche Scientifique de Belgique under grant number 2.5020.11 and by the Walloon Region.

***e*-Xtra:** Supplementary material is available online.

The author(s) declare no conflict of interest.

Rhizomania is a major disease of sugar beet, caused by the type member of genus *Benyvirus* in family *Benyviridae* (Gilmer and Ratti 2017), *Beet necrotic yellow vein virus* (BNYVV), a multipartite single-stranded RNA virus. BNYVV is transmitted by the plasmodiophorid protist *Polymyxa betae* Keskin (Decroës et al. 2019; Tamada and Asher 2016), an obligate intracellular parasite of *Beta vulgaris* roots, allowing the virus survival in soils, as resting spores, for decades. *P. betae* is also vector for other beet RNA viruses, namely, beet soil-borne mosaic virus (Heidel et al. 1997; Lee et al. 2001), beet soil-borne virus (BSBV) (Mahillon et al. 2021), and probably also beet virus Q (Crutzen et al. 2009). Two other species of the Plasmodiophorida order can also transmit specifically plant viruses, *Spongospora subterranea* is the vector of *Potato mop-top virus* (Jones and Harrison 1969; Reavy et al. 1998) and *P. graminis* is the vector of some *Beny-* (Bagayoko et al. 2021), *Bymo-* (Vaïanopoulos et al. 2006), *Furo-* (Vaïanopoulos et al. 2005), and *Pecluviruses* (Dieryck et al. 2009) associated with major diseases, mainly on cereals (Dieryck et al. 2011). On the other hand, no report relates viral transmission by *Plasmodiophora brassicae*, the type member of the plasmodiophorids, causal agent of clubroot of crucifers. At the physiological level, *Plasmodiophora brassicae* and *S. subterranea* induce the formation of galls in their host roots, whereas the infection by virus-free *Polymyxa* spp. remains asymptomatic. However, the induction of lateral root proliferation is observed following transmission of BNYVV (Peltier et al. 2011; Schmidlin et al. 2008). Both phenomena, galls formation and lateral roots proliferation, involve auxin biosynthesis and the signaling pathway in conjunction with plant defense, with upregulation of defense-related transcription factors (TF), pathogenesis-related (PR) proteins, and secondary phenolic compounds production (Fernando Gil et al. 2020; Malinowski et al. 2019).

There are only a few transcriptome profiling studies of the interactions between *Polymyxa* spp. and their hosts. McGrann et al. (2007, 2009) found a similar basal response to host and nonhost interactions of *P. betae* and *P. graminis* with sugar beet and barley, suggesting that resistance to *Polymyxa* spp. is not governed by pathogen-triggered immunity. Genes encoding for PR1a, PR5, cysteine proteases, a chitinase, a glutathione-*S*-transferase (GST), lipid transfer proteins, thionins, xyloglucan endo-transglycosylases (XTH), and extensin-like proteins were found among induced transcripts in early infection (McGrann et al. 2009). Two *B. vulgaris XTH* genes were reported to be involved in repairing cell wall damages caused by *P. betae* infection (Dimmer et al. 2004; Mutasa-Gottgens et al. 2000). Later, Desoignies et al. (2014) recorded 120 sugar beet

expressed sequence tags upregulated during the life cycle of *P. betae*. The transcriptomic profiling of 11 sugar beet genes revealed an active defense response, that began after 1 day and peaked after 5 days, during plasmodial growth. After 15 days, when zoosporangia and sporosori are formed, the plant response seemed quieter, as if *P. betae* was "immunitary hidden".

Much more attention was given to comparative transcriptomic studies of the interaction between the BNYVV and different hosts the virus is able to infect, like *B. vulgaris*, *B. macrocarpa*, or *Nicotiana benthamiana* (Fan et al. 2014, 2015a; Fernando Gil et al. 2020; Liu et al. 2017; Schmidlin et al. 2008), but most of these studies were focused on the virus-plant interaction in the absence of *P. betae*. Such studies systematically highlighted a major role of auxin in root disease development, activation of PR proteins, providing a better understanding of the BNYVV interaction with the sugar beet. Peltier et al. (2011) even showed the effect of the expression of the BNYVV p25 on hormonal changes and a root phenotype in *Arabidopsis thaliana*.

Yet only the seminal study by Schmidlin et al. (2008) analyzed both the BNYVV in *B. vulgaris* as well as in *B. macrocarpa* as host plants, providing information in the presence or the absence of the vector *P. betae*. Comparison of differential expression patterns in both *B. vulgaris* and *B. macrocarpa* concluded in genes differentially expressed in these hosts possibly because of the presence of *P. betae* in *B. vulgaris*.

The availability of sequenced accessions for both *B. vulgaris* (Dohm et al. 2014) and *P. betae* (Decroës et al. 2022) now provides the opportunity to improve our understanding of the tripartite interaction occurring between *B. vulgaris*, *P. betae*, and BNYVV by transcriptomic analysis. The scarcity of studies in this field also reflects the difficulty of simultaneously handling *P. betae* and BNYVV under fully controlled soil-free assay conditions (Kanyuka et al. 2003), for which a protocol is proposed to study interactions in the rhizomania pathosystem, using genetically characterized organisms. Results are discussed in light of the previous transcriptomic analysis of the plant-BNYVV and plant–*Plasmodiophora brassicae* interactions.

RESULTS AND DISCUSSION

Overview of RNA-seq data.

In the field, plant infection by BNYVV strictly requires *P. betae*, as there is no other known natural mode of transmission (Tamada 2016). It is, therefore, of interest to use the vector when studying plant-virus interactions under natural inoculation conditions (Tamada et al. 2021). Here, a new protocol aiming to reproduce BNYVV transmission by *P. betae* zoospores to sugar beet was optimized in a soil-free system, including exclusively genetically characterized organisms. This protocol was used to perform a comparative transcriptome analysis of the entire root system of sugar beets 28 days after inoculation with virus-free or virus-transmitting *P. betae* zoospores. Between 37.0 and 59.6 million good-quality read pairs were obtained in each of the 16 sequenced libraries. The percentages of mapped reads on the *P. betae* reference genome ranged from 14.4 to 34.3%. They ranged from 61.4 (in the presence of *P. betae*) to 98.1% (on mock-inoculated plants) on the *B. vulgaris* genome (Supplementary Table S1). In comparison with mock-inoculated plants, the differential expression analysis revealed twice as many genes influenced by inoculation of viruliferous *P. betae* (2,192) than with *P. betae* alone (1,002, mostly downregulated). Numbers of up- and downregulated genes for each comparison are summarized in a Venn diagram in Figure 1.

Kyoto Encyclopedia of Genes and Genomes (KEGG) categorization of potential differentially expressed gene (DEG) functions revealed that more pathways were significantly enriched in the presence of the virus than with *P. betae* alone, including pathways related to signaling, zeatin biosynthesis, as well as secondary metabolite synthesis (Table 1). Glutathione metabolism was the most enriched pathway in plants infected with *P. betae* alone and, to a lesser extent, with the virus. Seven of the enriched pathways in the presence of BNYVV (P value < 0.01) (Table 1) were already reported in a previous RNA-seq study using BNYVV without its vector on *B. vulgaris* (Fernando Gil et al. 2020), confirming the reliability of the RNA-seq data generated in the present work.

The expression changes of 10 target genes in each inoculation condition (*P. betae* alone or *P. betae* together with BNYVV vs. control), measured by RNA-seq and reverse transcription quantitative PCR (RT-qPCR), were highly correlated ($R^2 = 0.91$), further supporting RNA-seq data and analysis (Supplementary Fig. S1). More detailed bioassay results as well as an overview of RNA-seq statistics and mapping percentages are available in Supplementary Notes.

Since available annotation of the *P. betae* draft genome greatly rests on *in silico* predictions, an assembly of transcriptome sequences was performed in this study and was integrated with the initial annotation. As a result, 20,297 transcripts were reported belonging to 11,872 genes. Protein-coding genes were then annotated and their expression levels (measured in transcripts per million) and regulation were monitored in the presence or absence of BNYVV. Unfortunately, only 165 DEGs (93 up- and 72 downregulated) (Supplementary Table S2) were found without applying a fold-change threshold, probably due to high variability between replicates. The high sample dispersion found by multidimensional scaling analysis of gene expression data illustrates this high variability (Supplementary Fig. S2). To carefully exploit these results, we have chosen to focus only on significantly regulated genes, showing log-fold changes superior to 1 (64 genes).

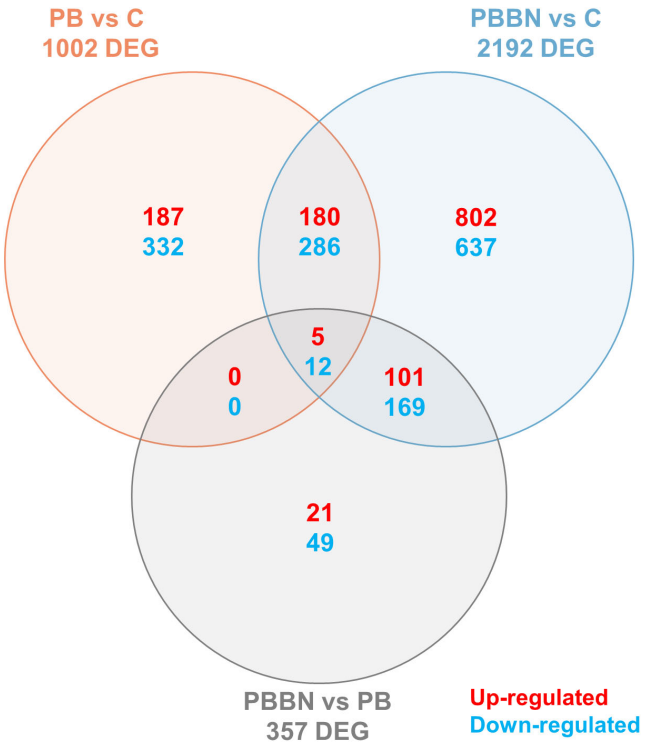

Fig. 1. Venn diagram showing the total of up- and downregulated *Beta vulgaris* genes between the three inoculation modalities. C = mock-inoculated plants, PB = plants infected with *Polymyxa betae* alone, PBBN = plants infected with *P. betae* and the beet necrotic yellow vein virus, and DEG = differentially expressed genes. Each circle represents one side of the three-way comparison. The number of up- and downregulated genes is shown in red and blue, respectively.

A detailed description of the main transcriptomic changes induced by inoculation with, on one hand, *P. betae* alone, and, on the other hand, *P. betae* and BNYVV is presented in the following sections, according to their putative effect on the plant.

The *P. betae* life cycle in sugar beet roots is influenced by the presence of BNYVV.

In rhizosphere, free *P. betae* zoospores enter sugar beet roots by infecting epidermal cells, preferably through roots hairs. Consequently, when the taproot starts enlarging, new infections occur essentially in thin lateral roots, bearing root hairs. The main symptom induced by BNYVV is precisely the proliferation of those lateral roots, which is likely an advantage for *P. betae* in later infection stages. During our experiments, no pronounced lateral root proliferation was observed yet, even though weak root proliferation was observed in some samples infected with the BNYVV. However, significantly higher relative *P. betae* DNA quantities were measured in plants infected with BNYVV than in plants inoculated with aviruliferous *P. betae*, at 1, 7, and 14 days postinoculation (dpi) (Fig. 2A). At 28 dpi, a higher relative quantity of *P. betae* DNA was measured in plants inoculated with *P. betae* alone than in the presence of BNYVV. On the one hand, this higher relative quantity at 28 dpi was confirmed by comparing the percentages of RNA-seq reads mapped to the *P. betae* reference genome (Fig. 2B) and by the higher relative level of *P. betae* internal transcribed spacer 1 (*ITS1*) transcripts measured by RT-qPCR in two independent bioassays (Fig. 2C). On the other hand, a greater number of sporangia and sporosori was observed after 14 days in the roots infected with *P. betae* together with BNYVV compared with *P. betae* alone–infected roots in both the upper part and the middle part of the roots. The same observation was made in the upper part of the roots at 28 dpi (Fig. 2D). Therefore, the *P. betae* life cycle seems to be accelerated in roots infected by the virus. Once entering the survival stage (sporosori), the multiplication of *P. betae* slowed down while root growth continued, thus explaining the lower *P. betae* relative quantity measured at the later timepoint. This effect could also explain the observation of similar sporosori relative quantities with and without BNYVV in the middle part of the roots at the same timepoint. We should note that the plant tissues taken at 14 and 28 dpi for visual observation differ between the two timepoints, as root length increased and new lateral roots were probably formed between the two sampling times. On a molecular level, strikingly, *P. betae* genes encoding homologs to Yippee-like protein, involved in conidiation in the rice blast pathogen *Magnaporthe oryzae* (Han et al. 2018), and to the conidiation-specific protein 10, a stress-responsive gene expressed during conidiation in the ascomycota *Neurospora crassa* (Shrode et al. 2001) were up-regulated in the presence of BNYVV. These findings endorse the hypothesis that *P. betae* enters earlier into the resting spore stage in roots co-inoculated with the virus. Similarly, the upregulation of *P. betae* genes involved in cell signaling (serine/threonine protein kinase activity), regulation of translation (Pumilio homolog 12), proteolytic activity (cathepsin-like, two metalloproteases), and other hydrolytic activities (lysosomal acid phosphatase, β-lactamase) could also be involved in the switch from the sporangial stage to the sporogenic stage of the life cycle of the protist (Supplementary Table S2). In addition to the induction of lateral root proliferation, our results suggest that the presence of BNYVV would also be beneficial to *P. betae* during early infection and root colonization. Similarly, Gerik and Duffus (1988) reported greater infection levels on sugar beets inoculated with BNYVV-carrying *P. betae* isolates when compared with the same isolates without the virus, and this for five of the six monosporosorus isolates tested.

The *P. betae*–induced genes related to oxidative stress management.

A strong impact of *P. betae* inoculation on the glutathione metabolism was observed in KEGG enrichments, independently of BNYVV. DEGs involved in redox regulation in plants were categorized using MapMan4 and were visualized on heatmaps to further explore this result (Fig. 3). *P. betae* infection induced significant upregulation genes coding for 17 or 15 GSTs in the presence or absence of BNYVV, respectively. Plant *GST* genes are known to be expressed under biotic and abiotic stress (Gullner et al. 2018) and *GST* upregulation has been seen in *A. thaliana* upon infection by *Plasmodiophora brassicae* (Irani et al. 2018), suggesting an important role for these enzymes in plant-plasmodiophorid interactions. Interestingly, such massive regulation was not reported in previous RNA-seq studies on

Table 1. Kyoto Encyclopedia of Genes and Genomes (KEGG) pathway enrichments in one or both up- and downregulated differentially expressed genes from *Polymyxa betae* alone and *P. betae* + beet necrotic yellow vein virus (BNYVV)-infected plants in comparison with mock-inoculated plants[a]

	PB vs. C		PBBN vs. C	
KEGG pathway	***P* value up**	***P* value down**	***P* value up**	***P* value down**
Glutathione metabolism	5.61E-16	–	3.65E-08	–
Metabolic pathways	9.19E-05	–	4.77E-09	–
Phenylpropanoid biosynthesis	–	–	1.14E-05	–
Biosynthesis of secondary metabolites	–	–	1.22E-05	–
Nitrogen metabolism	–	1.95E-05	–	1.57E-05
MAPK signaling pathway - plant	–	–	3.47E-05	–
Flavonoid biosynthesis	–	–	3.71E-05	–
Cyanoamino acid metabolism	–	–	4.20E-05	–
Zeatin biosynthesis	–	–	7.87E-05	–
Isoquinoline alkaloid biosynthesis	–	–	1.38E-04	–
Tyrosine metabolism	–	–	1.32E-03	–
Amino sugar and nucleotide sugar metabolism	–	–	2.10E-03	–
Carotenoid biosynthesis	–	–	–	6.35E-03
Pentose and glucuronate interconversions	–	–	7.96E-03	–
Circadian rhythm - plant	–	–	8.62E-03	–
Proteasome	3.01E-04	–	–	–
Ascorbate and aldarate metabolism	7.08E-04	–	–	–
Ribosome	2.69E-03	–	–	–

[a] Pathways are classified from the most significant to the least significant. Only *P* values below 0.01 are shown. Pathways in italics were previously reported, in a study by Fernando Gil et al. (2020), using full-length infectious cDNA clones of BNYVV. PB = *P. betae* alone, C = mock-inoculated control plants, and PBBN = *P. betae* + BNYVV.

BNYVV-plant interactions without the vector (Fan et al. 2014, 2015a; Fernando Gil et al. 2020) but was observed by Schmidlin et al. (2008) on *B. vulgaris* infected with BNYVV and *P. betae*. This effect on plants could therefore be attributed to *P. betae* and illustrates the importance of considering the vector when studying rhizomania pathosystems. In the current study, two putative *GST* genes were found in the 20 most expressed *P. betae* genes, further indicating that GST activity is crucial for the protist. The implication of GSTs in *P. betae–B. vulgaris* and in *Plasmodiophora brassicae–B. napus* interactions was already suggested by Mutasa-Gottgens et al. (2000) and Fei et al. (2015), respectively. Other plant genes related to redox homeostasis encoding glutaredoxins and ascorbate peroxidases were significantly up-regulated by *P. betae* alone or with BNYVV as compared with mock-inoculated plants. Thioredoxin genes were significantly up-regulated only in plants inoculated with *P. betae* alone. One NADPH-oxidase (Rboh) gene involved in H_2O_2 production was significantly down-regulated by both agents, especially without BNYVV. Interestingly, *P. betae* genes possibly linked to oxidative stress response (coding for one catalase involved in H_2O_2 decomposition, two HSP20, and one AhpC/thiol-specific antioxidant domain–containing protein) were also up-regulated in the presence of BNYVV. Furthermore, it was recently reported that several effectors of *Plasmodiophora brassicae* were able to suppress plant cell death activation associated with H_2O_2 accumulation and induced by other *Plasmodiophora brassicae* secretory proteins or by the mouse BAX protein (Chen et al. 2019). These findings highlight the importance of the control of oxidative stress for successful plant infection by plasmodiophorid obligate endoparasites. Altogether, redox homeostasis adjustments seem essential in *P. betae–B. vulgaris* compatible interaction and the alleviation of oxidative stress in the presence of *P. betae* could be beneficial for BNYVV, as previously proposed by Schmidlin et al. (2008).

Effect of *P. betae* and BNYVV on defense-related gene expression.

In this study, we found that more than 30% of the poly(A)-RNA extracted from sugar beet roots infected with *P. betae* alone originated from the latter. Despite this huge proportion,

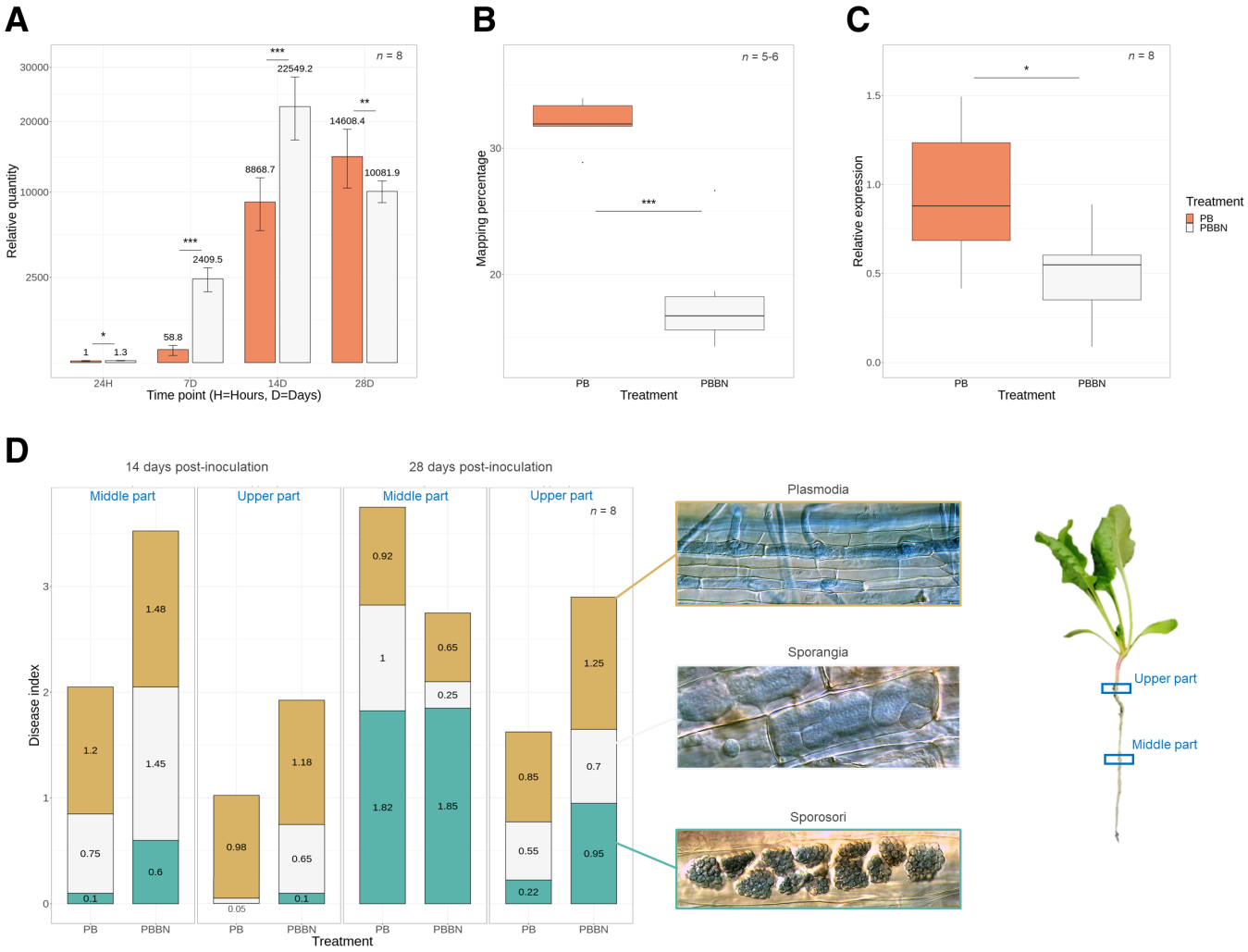

Fig. 2. Relative quantification of *Polymyxa betae* in sugar beet roots in three successive bioassays and visual assessment of *P. betae* life cycle in sugar beet roots. **A,** Bar chart of relative quantity of *P. betae* DNA normalized to *Beta vulgaris* DNA obtained by quantitative PCR (qPCR) ($n = 8$). **B,** Boxplot representation of percentages of mapped reads on *P. betae* A26-41 reference genome ($n = 5$ to 6). **C,** Boxplot representation of the relative quantity of *P. betae* ITS1 rRNA expression obtained by reverse transcription qPCR ($n = 8$). **D,** Stacked bar chart of the visual assessments of three *P. betae* structures (i.e., sporosori, sporangia, and undifferentiated plasmodia) at two different timepoints (14 and 28 days postinoculation) and in two parts of the root system (top and middle) (scale from 0 to 5 with 1 meaning <10% cells infected by a particular development stage, 2 = 10 to 30% cells infected, 3 = 30 to 50% cells infected, 4 = 50 to 70% cells infected, and 5 indicating >70% cells infected). C = mock-inoculated plants, PB = plants infected with *P. betae* alone, PBBN = plants infected with *P. betae* and the BNYVV. Significantly different levels were determined by *t*-test (one asterisk [*] indicates $P \leq 0.05$ and three [***] $P \leq 0.001$).

no symptoms were visible on plants one month after inoculation. Desoignies et al. (2014) reported that the sugar beet defense response to an established *P. betae* infection (when all life stages are present) was very weak, in comparison with earlier timepoints (Desoignies et al. 2014; McGrann et al. 2007). Conversely, several studies found a clear induction of sugar beet defenses after inoculation with BNYVV (Fernando Gil et al. 2020; Larson et al. 2008; Schmidlin et al. 2008; Webb et al. 2015, 2020). To gain insights into the differences between defense response to *P. betae* alone or carrying BNYVV, the expression of plant PR and PR-like protein genes was systematically monitored (Table 2). Our results confirmed the weak sugar beet defense reaction to the inoculation with *P. betae* alone, in comparison with the changes previously reported in *Plasmodiophora brassicae*–plant transcriptome analyses (Irani et al. 2018; Jia et al. 2017; Siemens et al. 2006). The presence of the protist especially influenced PR-9 (peroxidases, mostly induced), PR-10 (ribonuclease-like proteins, repressed), and PR-15-16 (oxalate oxidases and oxalate oxidases-like, repressed) families. A much stronger increase in the expression of PR and PR-like encoding genes was observed in the presence of BNYVV (17 down- and 71 upregulated DEGs) compared with *P. betae* alone (15 down- and 25 upregulated DEGs), including three *PR-1-type* genes represented in the top 20 of the most-upregulated genes in *P. betae* together with BNYVV plants (the Top 20 are reported in Supplementary Tables S3 and S4). Although induction of plant PR proteins by viral infection has been known for decades (Bol et al. 1990) and has been already reported for BNYVV (Fan et al. 2015a; Fernando Gil et al. 2020), our analysis reveals that this upregulation could also affect *P. betae*. In particular, several genes encoding putative endo-1,3-beta-glucosidases (PR-2) and chitinases (PR-3,4,8,11) were strongly up-regulated. Such induction was previously proposed to be involved in resistance against *P. betae* (Burketová et al. 2003) and *Plasmodiophora brassicae* (Zhang et al. 2016).

Similarly, KEGG pathways associated with biosynthesis of secondary metabolites were only significantly enriched among DEGs found in the presence of BNYVV. The tyrosine

Table 2. Differentially expressed genes belonging to pathogenesis-related (PR) proteins encoding PR and PR-like genes in response to *Polymyxa betae* with or without beet necrotic yellow vein virus (BNYVV)[a]

		PB vs. C			PBBN vs. C		
PR families	**No. genes**	**Down**	**Up**	**Total**	**Down**	**Up**	**Total**
PR-1	15	1	2	3	1	7	8
PR-2	36	0	0	0	0	7	7
PR-3	10	0	0	0	0	5	5
PR-4	2	0	0	0	0	1	1
PR-5	20	1	1	2	2	6	8
PR-6	2	0	1	1	1	1	2
PR-7	22	1	0	1	2	1	3
PR-8	9	0	1	1	0	3	3
PR-9	83	10	7	17	7	13	20
PR-10	8	0	3	3	0	4	4
PR-11	3	0	0	0	0	2	2
PR-12	2	0	0	0	0	1	1
PR-13	0	0	0	0	0	0	0
PR-14	4	0	0	0	1	0	1
PR-15-16	52	2	9	11	3	19	22
PR-17	3	0	1	1	0	1	1
Total	271	15	25	40	17	71	88

[a] Genes are listed in detail in Supplementary Table S5. Significant up- (up) and downregulation (down) in comparison with mock-inoculated plants are summarized. PR and PR-like were identified through tBLASTn searches on *B. vulgaris* refseq_rna (E-value $< e^{-6}$). C = mock-inoculated plants, PB = plants infected with *P. betae* alone, PBBN = plants infected with *P. betae* and BNYVV.

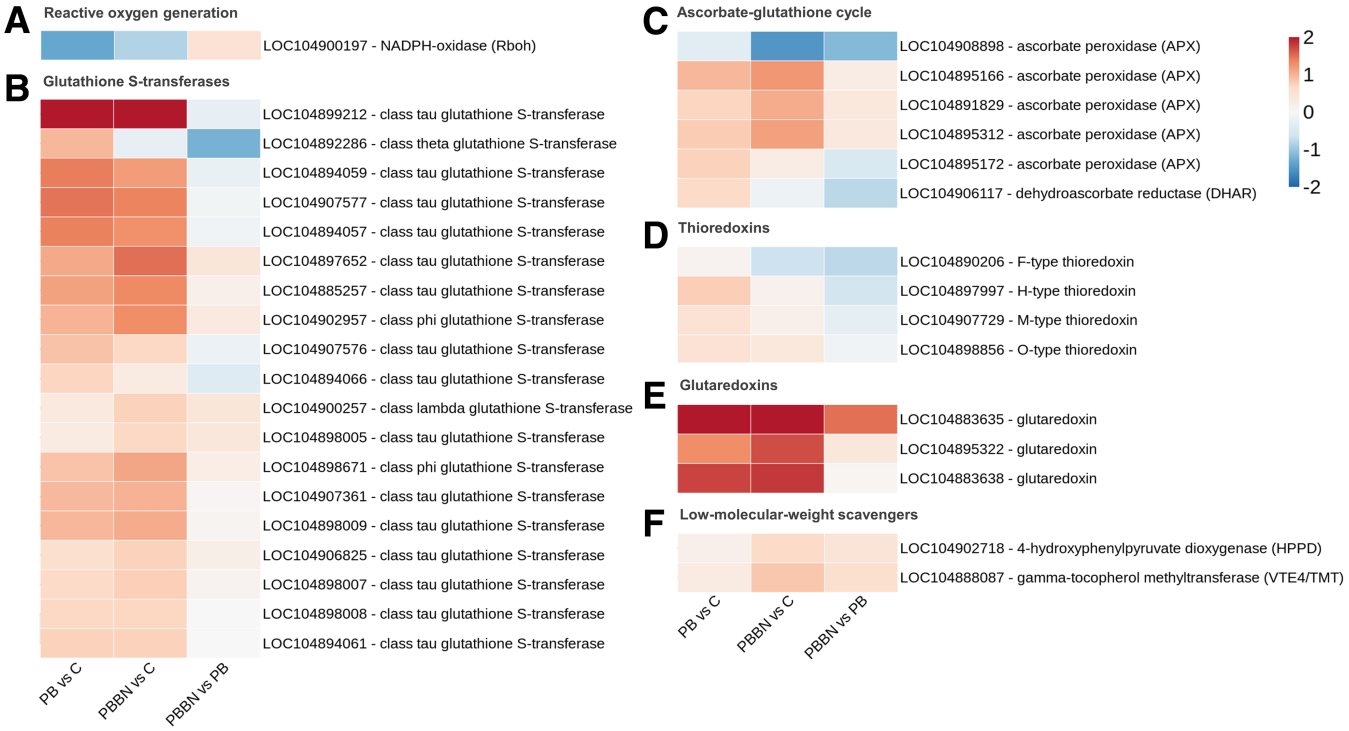

Fig. 3. Redox homeostasis in response to *Polymyxa betae* with or without beet necrotic yellow vein virus (BNYVV) inoculation. **A,** Heatmaps of differentially expressed genes related to reactive oxygen generation, **B,** glutathione-*S*-transferase activities, **C,** ascorbate-glutathione cycle, **D,** thioredoxins, **E,** glutaredoxins and **F,** low–molecular weight scavengers are shown. Up- and downregulation are represented in red and blue, respectively. The scale is based on $\log_2$ fold changes. C = mock-inoculated plants, PB = plants infected with *P. betae* alone, and PBBN = plants infected with *P. betae* and the BNYVV. Genes were classified according to Mercator/MapMan4. Annotations comprised the National Center for Biotechnology Information Gene symbol and the MapMan4 annotation.

pathway, potentially acting upstream to flavonoid and phenylpropanoid pathways, was induced. Phenylpropanoid, flavonoid, and dopamine pathways were also globally stimulated, as represented on KEGG maps in Supplementary Figures S3 and S4. Accordingly, all genes belonging to the LNK (night light–inducible and clock-regulated) family were significantly down-regulated only in the presence of BNYVV. LNK 1 and LNK 2 are known to be co-repressors of the phenylpropanoid pathway in *A. thaliana* (Zhou et al. 2017). Their repression in sugar beet probably coincides with the activation of the phenylpropanoid pathway. Flavonoid metabolism genes were further classified using MapMan4 (Supplementary Fig. S5). Most of them were up-regulated, mainly in the presence of BNYVV, including two *chalcone synthases*, a *chalcone isomerase*, a *shikimate O-hydroxycinnamoyltransferase*, and five *aureusidin synthases*. The activation of the flavonoid pathway and the accumulation of flavonoids was previously documented in the rhizomania pathosystem (Fernando Gil et al. 2020; Webb et al. 2020) and during gall formation by *Plasmodiophora brassicae* on *A. thaliana* (Päsold et al. 2010). As observed here with *P. betae* and BNYVV, biosynthetic pathways downstream of the shikimic acid were also reported to be up-regulated by *Plasmodiophora brassicae*, including *chalcone synthases*. These observations could be related to the accumulation of antioxidants and antimicrobials (Dao et al. 2011; Irani et al. 2018). Overexpression of *aureusidin synthases* is probably involved a plant reaction against BNYVV, as aurones have been shown to inhibit viral replication (Haudecoeur et al. 2011).

Other sugar beet genes encoding antimicrobial proteins were influenced by the inoculation, such as a polygalacturonase-inhibiting protein (PGIP) upregulated solely in *P. betae* together with BNYVV, suggesting that the plant is trying to counteract cell wall–degrading enzymes (Kalunke et al. 2015). The downregulation of two antiviral protein alpha genes in *P. betae* alone and *P. betae* together with BNYVV could benefit BNYVV.

DEGs involved in pathogen detection and plant-defense regulation.

A distinct plant-defense response was observed in plants inoculated with *P. betae* alone or with BNYVV-carrying zoospores. Resistance gene analogues (RGAs) and TFs were systematically monitored to further evaluate the regulation of genes putatively involved in pathogen recognition and regulation of plant defenses (Table 3; Supplementary Fig. S6). The expression of 644 RGA genes were recorded in this study. When *P. betae* was inoculated alone, only four of these were significantly up-regulated compared with 58 that were down-regulated. Interestingly, some genes belonging to the wall-associated kinase (WAK) and WAK-like protein family were repressed. WAKs are thought to bind to pectin and could possibly have a role as cell wall "sensors" (Kohorn and Kohorn 2012). Genes encoding damage elicitor peptide (proPEP) and one TF involved in symbiosis signaling (ERN1) were also strongly down-regulated. The global repression of RGAs with *P. betae* alone suggests that the protist would be able to hijack host cell metabolism and that defense signaling pathway repression likely plays a central role. An increasing number of effectors of *Plasmodiophora brassicae* have been reported in recent years (Bulman et al. 2018; Chen et al. 2019, 2021; Galindo-González et al. 2021; Hossain et al. 2021; Ludwig-Müller et al. 2015; Pérez-López et al. 2020, 2021; Yu et al. 2019). In previous work, we also reported some *P. betae* predicted proteins putatively involved in plant-defense interference, such as ankyrin-containing proteins, PR-4 homologs, and isochorismatases (Decroës et al. 2022). Like *Plasmodiophora brassicae*, it is highly probable that *P. betae* uses effectors to suppress plant defenses. Their precise localization and action should be further investigated. However, when BNYVV was transmitted, 30 RGAs were significantly induced (vs. 49 repressed), including genes encoding eight membrane receptor–like kinases (RLK) (leucine-rich repeat [LRR]-transmembrane [TM]-serine-threonine kinase [STK]), 14 cytosolic STKs (Pto), four RLK-like proteins (RLP) (LRR-TM), and one CNL (coiled coil-nucleotide binding site-LRR). *Brassinosteroid insensitive 1–associated receptor kinase* (*BAK1*) was significantly up-regulated solely in the presence of BNYVV. These results reflect the stronger plant-defense reaction when BNYVV is added to the pathosystem. Here, *P. betae* genes encoding one ankyrin-rich protein as well as proteases and other hydrolases were also up-regulated in the presence of BNYVV (Supplementary Table S2). These proteins could be involved in *P. betae–B. vulgaris* interaction through the catabolism of host compounds (Jashni et al. 2015).

The presence of *P. betae* and BNYVV also influenced the expression of genes encoding TF. A summary of up- and down-regulated TF families known to intervene with plant defenses is presented in Table 4. Consistent with the results for RGA and PR genes, TF expression was more strongly affected in plants infected with the virus than with *P. betae* alone. TF from the AP2/ERF, WRKY, and bHLH families were particularly influenced when BNYVV was transmitted. Notably, only four down-regulated WRKY were found with *P. betae* alone, whereas nine were up-regulated in the presence of BNYVV. TF from the MYB

Table 3. Differentially expressed genes belonging to resistance genes analogues (RGAs) in response to *Polymyxa betae* with or without beet necrotic yellow vein virus (BNYVV)[a]

		PB vs. C			PBBN vs. C		
RGA groups	**No. genes**	**Down**	**Up**	**Total**	**Down**	**Up**	**Total**
Coiled coil-nucleotide binding site-leucine-rich repeat (CC-NBS-LRR)	27	4	0	4	4	1	5
Toll/interleukin-1 receptor-NBS-LRR	1	0	0	0	0	0	0
Receptor-like kinases (RLK)	128	5	0	5	10	8	18
RLK-like proteins	45	2	0	2	6	4	10
Cytosolic serine-threonine kinase	335	24	4	28	13	14	27
Ntir	2	1	0	1	0	0	0
Nltir	8	2	0	2	1	0	1
Nlcc	39	8	0	8	7	1	8
Ncc	15	1	0	1	2	1	3
CC-NBS	21	5	0	5	3	0	3
Additional putative RGAs without specific domains in exons	23	6	0	6	3	1	4
Total	644	58	4	62	49	30	79

[a] Significant up- (up) and down-regulation (down) in comparison with mock-inoculated plants are summarized. RGAs were identified and classified by Dohm et al. (2014) according to the presence of domains known to be involved in resistance to pathogens (Supplementary Fig. S6; Supplementary Table S6). PB = plants infected with *P. betae* alone, C = mock-inoculated plants, and PBBN = plants infected with *P. betae* and BNYVV.

superfamily members also showed distinct regulation patterns depending on the infection with *P. betae* and BNYVV.

The hormonal modulation underlying the activation of plant defenses in the presence of BNYVV remains ambiguous. Jasmonate synthesis and signal transduction pathways were poorly influenced by inoculation. Salicylic acid (SA) signal transduction and ethylene biosynthesis pathway and response seem to be induced in the presence of BNYVV (Supplementary Fig. S7). This is consistent with the activation of multiple *PR-1* and *endochitinase* genes. Notably, four plant *SAMT* genes, coding for enzymes involved in SA modification to its inactive methyl salicylate form (MeSA), were repressed in the presence of BNYVV and, to a lesser extent, with *P. betae* alone. The activation of a *SA-binding protein 2* (*SABP2*) gene, responsible for the conversion of MeSA into SA (Forouhar et al. 2005), was also observed with BNYVV. It was demonstrated that a secreted methyltransferase produced by *Plasmodiophora brassicae* (PbBSMT) contributes to the susceptibility of *A. thaliana* to this plasmodiophorid through metabolization of SA in its methylated volatile form (Bulman et al. 2018; Ludwig-Müller et al. 2015). However, no homolog of *PbBSMT* was found in the *P. betae* draft genome (Decroës et al. 2022). The reduction of SA methylation could induce a progressive local accumulation of SA, which would, in turn, increase defenses in plant roots. Accordingly, the *TGA4* gene, thought to encode a repressor of SA defenses responses (Foley and Singh 2004), was also repressed.

Altogether, it seems that *P. betae* alone is able to suppress plant defenses but that a strong plant reaction occurred in the presence of BNYVV. Once a certain threshold is reached, the stress induced by plant-defense reaction may have a detrimental effect on *P. betae*, forcing the protist to switch to its resting spore life stage. Supporting this hypothesis, we observed that the induction of plant defenses was maximal after 14 days, at the same time as the switch to the survival stage of *P. betae* that occurred mainly in BNYVV-infected plants. This agrees with early observations that BNYVV preinfection inhibited subsequent development of *P. betae* in sugar beet (Prillwitz and Schlösser 1992; Schlösser 1990). However, it should be noted that faster early root invasion by the protist in the presence of BNYVV could also result in a lack of available free cells (not already containing *P. betae* structures) or resources to support further *P. betae* multiplication. In this case, the protist is expected to enter the survival stage, as observed when roots are heavily infected (Legrève et al. 1998).

Table 4. Differentially expressed genes belonging to defense related transcription factor (TF) families in response to *Polymyxa betae* with or without beet necrotic yellow vein virus (BNYVV) inoculation[a]

	PB vs. C			PBBN vs. C		
TF genes	**Down**	**Up**	**Total**	**Down**	**Up**	**Total**
MYB	2	1	3	3	6	9
MYB-related	0	2	2	5	1	6
G2-like GARP	0	1	1	3	0	3
bZIP	2	1	3	4	2	6
TGA	0	0	0	1	0	1
BOP	0	0	0	1	0	1
ERF	1	1	2	0	8	8
DREB	1	0	1	3	2	5
AP2	0	0	0	1	3	4
NAC	2	1	3	5	5	10
WRKY	4	0	4	2	9	11
bHLH	4	1	5	10	5	15
TIFY	0	0	0	1	2	3
TPL/TPR	0	0	0	1	0	1
AFP/NINJA	0	0	0	1	0	1
Total	16	8	24	41	43	84

[a] A complete list can be found in Supplementary Table S7. Significant up- (up) and downregulation (down) in comparison with mock-inoculated plants are summarized. *TF* genes were classified according to MapMan4. PB = plants infected with *P. betae* alone, C = mock-inoculated plants, and PBBN = plants infected with *P. betae* and BNYVV.

Regulation of cell wall–related genes in response to *P. betae* and BNYVV infection.

Cell-wall remodeling is suspected to be involved in *P. betae*–sugar beet interaction (Desoignies et al. 2014). It is also known that BNYVV influences sugar beet genes associated with cell wall organization during auxin-triggered lateral root development (Fernando Gil et al. 2018, 2020). Heat maps of the major cell wall DEGs are proposed to illustrate the changes in tripartite interaction (Fig. 4). Cell wall synthesis–related transcriptome was mainly repressed in *P. betae*–infected roots compared with mock-inoculated roots (Fig. 4A). Transcripts related to proteins involved in cellulose synthase complex (CSC) (i.e., CSC-interactive protein and the catalytic component CesA), in hemicellulose synthesis (two glucuronosyltransferase and one xyloglucan galacturonosyltransferase), and in pectin synthesis (xylogalacturonan xylosyltransferase) were significantly down-regulated in comparison with mock-inoculated plants. Genes coding for enzymes involved in hemicellulose modification and degradation (endo-beta-1,4-mannanase/xylanase, xylan *O*-acetyltransferase) and in pectin modification and degradation, including pectin methylesterases and a beta-galactosidase, were also significantly repressed in the presence of *P. betae* alone (Fig. 4B). It was previously proposed that cell wall alterations involving induction of pectin methylesterase and expansins in *A. thaliana* are involved in *Plasmodiophora brassicae* gall formation (Agarwal et al. 2011; Devos et al. 2006; Irani et al. 2018). Cell-to-cell movement of *P. betae* is thought to happen either through the release of zoospores inside the roots, through myxamoeboid movement of the protist, or both (Barr and Asher 1996; Mithen and Magrath 1992; Tamada 2016). Both mechanisms are thought to rely on cell wall–degrading enzymes and could benefit from reduction of plant cell wall integrity. Here, several cell wall peroxidases (PR-9 family), known to be involved in cell wall lignification (van Loon et al. 2006), were also repressed in both inoculation conditions, especially with *P. betae* alone (Table 2). Moreover, extensin and cell wall glycoprotein–encoding genes were clearly down-regulated following infection with *P. betae* alone (Fig. 4C). Notably, three *extensin-1-like* genes were found in the top 20 of the most-downregulated genes with *P. betae* alone in comparison with mock-inoculated plants (Supplementary Table S4). Extensins were previously shown to be involved in cell wall strengthening and root defenses, notably against pathogenic oomycetes (Castilleux et al. 2020). These repressions could be key for *P. betae* root colonization. The repression of cell wall synthesis–related genes was less marked in plants infected with BNYVV, and several genes encoding enzymes involved in cell wall modification were induced, especially with regard to pectin modification and degradation. Three pectin acetyltransferase-, two pectin methylesterase-, and one polygalacturonase (QRT2)-encoding genes were significantly up-regulated. The expression levels of cell wall protein genes, such as some *expansins*, were also higher in the presence of BNYVV. The lateral root proliferation induced by BNYVV is initiated by the conversion of root cells into meristematic cells and involves the regulation of genes associated with cell wall organization (Fernando Gil et al. 2018, 2020). Known regulated genes include *pectin methylesterases*, *polygalacturonases*, and *expansins* with BNYVV alone (Fernando Gil et al. 2020) (Supplementary Table S3) and could influence cell wall biomechanical properties such as rigidity (Wormit and Usadel 2018). In particular, *expansins* were previously found to be up-regulated after BNYVV infection with or without the vector (Fan et al. 2015a; Fernando Gil et al. 2018; Schmidlin et al. 2008) as well as in BNYVV p25 protein–expressing transgenic *A. thaliana* roots

(Peltier et al. 2011) and are associated with cell wall loosening during root hair and lateral root formation (Cosgrove 2015). Taken together, these results highlight the probable importance of cell wall–remodeling enzymes and proteins in the *B. vulgaris*–*P. betae*–BNYVV interaction. The effect of BNYVV on cell wall organization, including the likely loosening of the cell walls, observed here and reported elsewhere (Fernando Gil et al. 2018, 2020) may have a beneficial effect for the development of *P. betae* in the roots. Alterations in the cell wall to the benefit of the plasmodiophorid was also suggested for *Plasmodiophora brassicae*, which does not transmit viruses but induces the formation of root galls (Devos et al. 2006; Malinowski et al. 2019).

Even though we did not observe transcriptional reprogramming of genes involved in RNA silencing, the possibility remains that *P. betae* would also benefit from the viral ability to suppress host RNA silencing, mediated by the RNA2-encoded P14 (Chiba et al. 2013), the noncoding RNA3 (Flobinus et al. 2016, 2018), and RNA4-encoded p31 (Rahim et al. 2007). The RNA-dependent RNA-polymerase 6 (RDR6) silencing pathway, thought to be targeted by P14 activity, was indeed previously reported to participate in defense against bacterial and fungal pathogens in rice (Wagh et al. 2016) and the upregulation of an *RDR6* homolog in sugar beet during *P. betae* early infection was reported by Desoignies et al. (2014).

The hormonal modulation underpinning changes in the expression of a cell wall–related gene was also investigated. DEGs involved in auxin and cytokinin balance were seen in our study (Supplementary Fig. S7). As reported by Fernando Gil et al. (2020), some genes involved in auxin synthesis from L-tryptophan (*YUCCA*, *tyrosine decarboxylase 1*, *aldehyde dehydrogenase*) were up-regulated in the presence of BNYVV and also with *P. betae* alone, although not *tyrosine decarboxylase 1*. Consistent with the study by Schmidlin et al. (2008), our results confirmed the upregulation of auxin-binding protein genes. Genes putatively involved in auxin transport (*PIN* and an *auxin transport regulator kinase* [*PINOID*]) were also up-regulated, but only in the presence of BNYVV. Conversely, three auxin efflux transporter genes from a PIN-like family (*PILS*) were repressed, especially in the presence of BNYVV. The influence of inoculation on auxin-related genes was expected, since lateral root proliferation induced by BNYVV was reported to be controlled by auxin signaling due to the interaction of the viral P25 virulence factor with the auxin/indole acetic acid protein BvAUX28 (Fernando Gil et al. 2018). Interestingly, overexpression of *PINOID* was found to trigger lateral root formation in *A. thaliana* mutants (Benjamins et al. 2001). On the other hand, PILS action was reported to decrease auxin signaling in *A. thaliana* roots. Moreover, *pils* knockout mutants displayed a higher density of lateral roots, while overexpression of *PILS* in root hairs led to a reduction of their growth (Barbez et al. 2012). The regulation of genes related to auxin transport by BNYVV could therefore be involved in the initiation of rhizomania symptoms. At the time of analysis, the "classical" cytokinin signaling pathway was repressed in the presence of both *P. betae* and BNYVV. As a matter of fact, *histidine-kinase receptors* (*AHK*) genes were not regulated and *AHP6*, encoding a repressor of AHK signaling, was induced. However, the cytokinin signaling pathway activator gene (*CKI1*) was strongly induced in both inoculation conditions. In *A. thaliana*, CKI1 activates similar cytokinin responses to AHK but in a cytokinin-independent manner and is regulated by light perception (Deng et al. 2010; Dobisova et al. 2017). The development of *Plasmodiophora brassicae* root

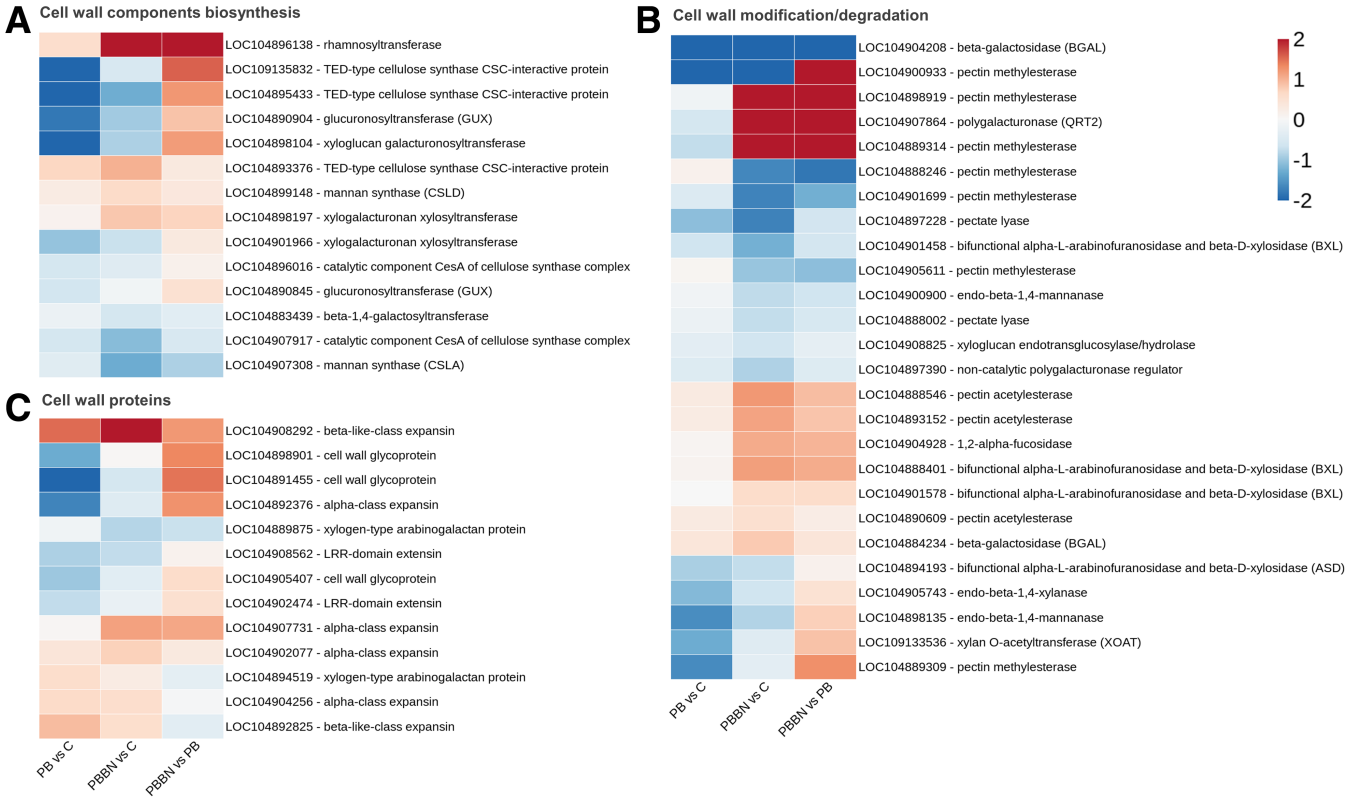

Fig. 4. Cell wall–related gene expression in sugar beet in response to *Polymyxa betae* with or without beet necrotic yellow vein virus (BNYVV) inoculation. **A,** Heatmaps of differentially expressed genes related to cell wall components biosynthesis, **B,** cell wall proteins, and **C,** cell wall modification and degradation are shown. Up- and downregulation are represented in red and blue, respectively. The scale is based on $\log_2$ fold changes. C = mock-inoculated plants, PB = plants infected with *P. betae* alone, and PBBN = plants infected with *P. betae* and BNYVV. Genes were classified according to Mercator/MapMan4. Annotations comprised the National Center for Biotechnology Information Gene symbol and the MapMan4 annotation.

galls is controlled by auxin and cytokinin pathways (Malinowski et al. 2019). Similarly, these pathways seem to be key in *P. betae*–BNYVV–sugar beet interaction.

Evidence for new physiological sinks in sugar beet roots.

The infection of *B. vulgaris* by *P. betae* results in the development of plasmodia, sporangia, and, eventually, thick-walled resting spores within host root cells. BNYVV infection leads, in natural conditions, to an abnormal production of lateral roots and a reduced sugar content in the taproot. Therefore, transcriptomic changes related to a reorganization of carbohydrate metabolism were expected in plants infected with *P. betae* and BNYVV. The setup of physiological sink tissues was already reported upon the attack of host plants by *Plasmodiophora brassicae*, which induces root cell proliferation during gall development (Malinowski et al. 2019; Siemens et al. 2011). In contrast, *P. betae* does not cause galls, and our study reveals that no meaningful reprograming of genes related to carbohydrate metabolism was observed upon infection with *P. betae* alone. On the other hand, clues of glucose shortage appeared in the presence of BNYVV (Supplementary Fig. S8). In particular, genes for key enzymes of the glyoxylate cycle, isocitrate lyase and malate synthase (MS), were also strongly up-regulated in the presence of *P. betae* and BNYVV. Only the malate synthase gene was significantly affected by virus-free *P. betae*. The activation of the glyoxylate cycle generally occurs when complex carbon sources are lacking and allows use of acetate originated from fatty acids (FA) beta-oxidation to produce glucose (Fan et al. 2015b; Lorenz and Fink 2002). One *SWEET* transporter gene and one sucrose transport protein gene were also significantly activated in the presence of the virus. Two genes encoding a cell wall invertase and a vacuolar invertase were slightly induced only in the presence of BNYVV, in comparison with mock-inoculated plants. Such regulation was previously reported as enhancing sugar supply from the phloem during the establishment of sink tissues (Tauzin and Giardina 2014) and could be linked to lateral root proliferation (Sergeeva et al. 2006). This effect may also contribute to the reduced sugar content in diseased *B. vulgaris* taproots (McGrann et al. 2009; Nieberl et al. 2017).

Lipid metabolism was also suspected to be influenced by infection. A recent metabolome profiling study showed a modulation of *B. vulgaris* root lipid composition following BNYVV and *P. betae* inoculation (Webb et al. 2020). Moreover, the induction of several plant FA synthesis and elongation–related genes was also reported in *A. thaliana* roots infected with *Plasmodiophora brassicae* (Irani et al. 2018). Accordingly, our results reveal that four and seven genes involved in FA synthesis were slightly induced in plants infected with *P. betae* alone and in the presence of BNYVV, respectively, whereas none were significantly repressed (Supplementary Fig. S9). Conversely, most DEGs involved in complex lipid synthesis, such as glycerolipids and phytosterols synthesis, were repressed, especially when BNYVV was present. Five phospholipase-related genes were significantly down-regulated in the presence of *P. betae* alone, whereas five were down-regulated (*PI-PLC* and *PLD-epsilon* in common) and two were up-regulated in plants inoculated with virus-transmitting zoospores. One lipid droplets (LD) biogenesis factor gene (*SEIPIN*) was also strongly repressed only in the presence of BNYVV. The repression of this gene can be linked to the fact that the mean fluorescence of plant root cells (free of *P. betae* structures), stained the LD-specific LD540 lipophilic fluorescent dye, appeared higher in mock-inoculated plants than in plants infected with *P. betae* and BNYVV (Fig. 5A). Meanwhile, a considerable number of LD were observed by confocal microscopy in all *P. betae* structures, especially sporangia, independently of the presence of the virus (Fig. 5B). The upregulation of some *P. betae* genes putatively involved in lipid metabolism (predicted to code for two lipases and two apolipoprotein domain–containing proteins) was, however, evident in the presence of BNYVV (Supplementary Table S2). Interestingly, LD organization seems to differ between *P. betae* life stages, being denser in sporangia and sporosori (Fig. 5B, sections e to h) than in earlier life stages (Fig. 5B, sections a to c). Abundant LD were previously observed in the exit tube

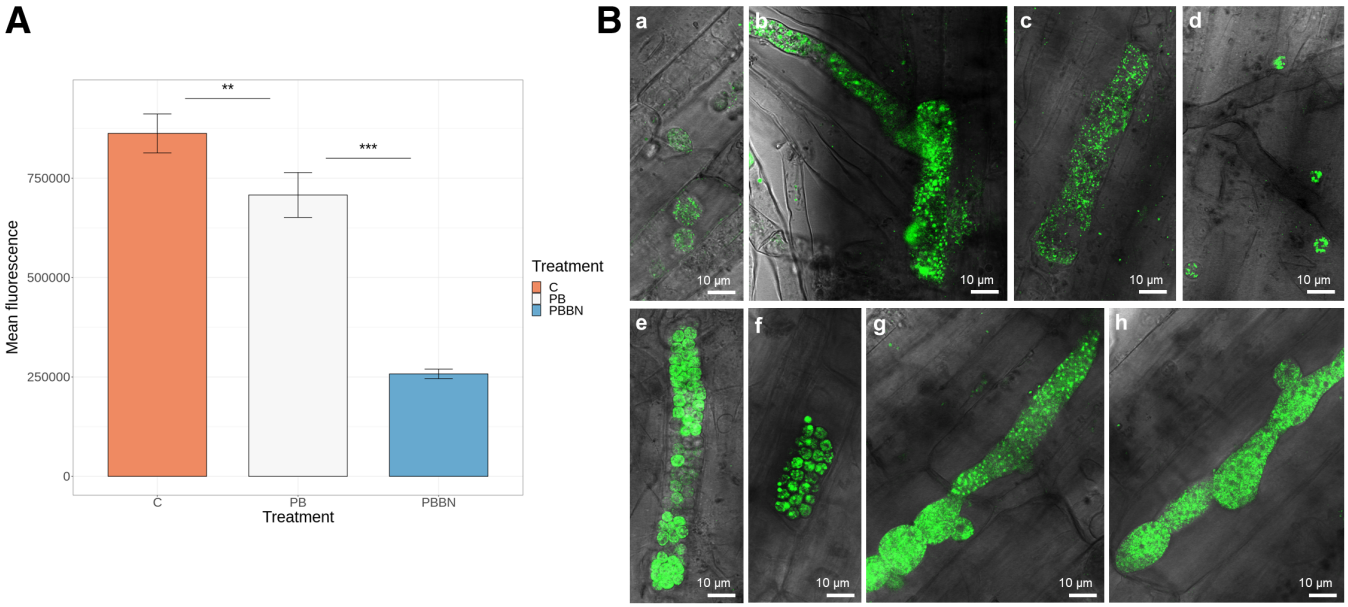

Fig. 5. A, Barplot of the mean fluorescence derived from lipid droplets (LD) in *Beta vulgaris*, and **B,** representative images of LD content observed in various *Polymyxa betae* life stages without beet necrotic yellow vein virus (BNYVV). Roots were stained in vivo with the LD-specific dye LD540 and were observed with a LSM710 confocal microscope. Data in A represent the means ± standard deviation ($n = 4$) and significantly different levels were determined by *t*-test (two asterisks [**] for $P \leq 0.01$ and three [***] for $P \leq 0.001$). C = mock-inoculated plants, PB = plants infected with *P. betae* alone, and PBBN = plants infected with *P. betae* and the BNYVV. *P. betae* structures visible in B are meronts (a), plasmodia (b, c), encysted secondary zoospores (d), sporosori (e, f), and zoosporangia (g, h).

of zoosporangia of *P. betae* (D'Ambra and Mutto 1977) as well as in zoospores of *P. graminis* (Barr and Allan 1982), in which they are supposed to play a role in germination and host infection (D'Ambra and Mutto 1977; Murphy 2012), but this is the first time that they are reported in all stages of life. Notably, the LD540 fluorescent dye appeared highly efficient to label *P. betae* LD and could be tested with other plasmodiophorids. The high content in LD is likely linked to energy storage in *P. betae*, that could be mobilized for membrane extension or in case of energy or carbohydrates shortage, as proposed for *Plasmodiophora brassicae* (Bi et al. 2016; Irani et al. 2019) and other fungi (Murphy 2012). In the latter, transcriptomic changes associated with lipid metabolism were also observed during resting spore formation (Schwelm et al. 2015; Bi et al. 2016). Here, the regulation of lipid metabolism–related genes in the plant and in *P. betae* coincides with a faster *P. betae* cycle, suggesting that similar mechanisms could occur in both plasmodiophorids. Whether *P. betae* is directly able to use host-derived FA or mainly produce its own from nutrients absorbed from host cells remains a question. Unlike *Plasmodiophora brassicae*, which probably depends on the plant for FA synthesis, since its genome lacks FA synthase genes (Schwelm et al. 2015), five putative FA synthase genes were found in the *P. betae* transcriptome. These genes are putatively involved in the lipid metabolic pathways.

Expression dynamics of selected sugar beet genes at four timepoints after the infection by *P. betae* alone and *P. betae* together with BNYVV.

The expression dynamics of selected genes involved in oxidative stress regulation and plant defenses was monitored 1, 7, 14, and 28 days after inoculation with *P. betae* with and without BNYVV in an independent assay (Fig. 6). Results showed a dynamic plant response depending on genes and treatments (presence or not of *P. betae* with or without BNYVV). Only a downregulation of one of these genes (one peroxidase, *BvPER44*) was observed after 24 h but a significant upregulation of most of the tested genes was initiated at 7 days, which peaked after 14 days in the presence of BNYVV and decreased later. Results obtained by qRT-PCR in this assay followed a similar trend than the results obtained in the RNA-seq analysis (e.g., *BvPR1a*, *BvGSTU*, *BvTPL1*, *BvSE2*, *BvRGA3*) with some exceptions (e.g., *BvAPX3*, *BvGRXS9*, *BvPER44*), possibly associated with environmental variations between both assays. Interestingly, the expression of *Rboh* and oxidative stress–response genes were systematically lower in plants inoculated with *P. betae* alone than with the virus-transmitting zoospores. The same trend was observed with the selected PR genes (*BvPR1a*, *BvTLP1*, *BvSE2*). This confirms that the presence of BNYVV is associated with a stronger activation of plant defenses, even in timepoints preceding the RNA-seq analysis.

MATERIALS AND METHODS

Biological material and bioassays.

Biological material and inoculum production. Two accessions of *Beta* spp. were used, namely, *Beta macrocarpa* and the double-haploid monogerm line KWS2320 of *B. vulgaris* that was fully sequenced by Dohm et al. (2014). Seeds were pregerminated on moistened germination paper (22°C, in the dark) and were transplanted in tubes filled with sterilized quartz sand. Tubes with *B. macrocarpa* and *B. vulgaris* KWS2320 were then placed in individual flow-through collecting pots, were daily amended with half-strength Hoagland solution (Hoagland and Arnon 1950), and were maintained in a growth cabinet at 20 and 25°C (night and day) with a 14-h photoperiod. Plants of *Chenopodium quinoa* were grown in individual pots filled with compost and were placed in a greenhouse in the same conditions.

The virus-free *P. betae* A26-41 monosporosorus-derived isolate, sequenced by Decroës et al. (2019), was multiplied in roots of *B. vulgaris* plants grown in an automatic immersion system, as described by Legrève et al. (1998), and were used to release zoospores as previously described (Desoignies et al. 2011).

BNYVV infectious clones pB15, pB214, pB35, and p45 containing, respectively, the complementary DNAs (cDNAs) for type B BNYVV RNAs 1, 2, 3, and 4 (Quillet et al. 1989; Ziegler-Graff et al. 1988) were used in bioassays. The initial BNYVV RNA inoculum was produced by in vitro transcription and was inoculated on *C. quinoa* leaves as described by Crutzen et al. (2009). After the appearance of symptoms (1 week), infected leaves were harvested and ground in phosphate buffer (50 mM KH_2PO_4, pH 7). The resulting sap was used for mechanical inoculation on *B. macrocarpa* leaves, using Carborundum as abrasive. Leaves from *B. macrocarpa* plants showing systemic symptoms (14 to 21 days after inoculation) were then ground in four volumes (wt/vol) of root inoculation buffer (50 mM KH_2PO_4, 30 g of Carborundum per liter, 1 g of Na_2SO_3 per liter, pH 7) and were mechanically inoculated onto the root systems of individual two-week-old *B. macrocarpa* seedlings, using a protocol adapted from Koenig and Stein (1990). Briefly, roots were individually vortexed two times for 30 s in inoculation sap with 30 s on ice in between. The conservation of the sap infectivity during the whole inoculation process was confirmed by mechanical inoculation of *C. quinoa* leaves. Mock-inoculated plants were obtained following the same procedure with a sap produced from healthy *B. macrocarpa* leaves. Plants were transplanted in tubes and were grown under controlled conditions (described above). Two weeks later, plants were inoculated with 1 ml of a suspension containing 10^4 virus-free *P. betae* zoospores. Virus-free plants were inoculated in the same way with *P. betae*, and other plants were mock-inoculated using a suspension produced from healthy sugar beet roots. After 3 weeks of growth, the *B. macrocarpa* were carefully extracted from the quartz sand, 30 to 50 mg of roots were sampled to check their inoculation status (presence or absence of *P. betae* and BNYVV) by RT-PCR (described below), and the plants were transplanted. After one more week, plants infected with both *P. betae* and BNYVV, plants with *P. betae* alone, and mock-inoculated plants were used to release zoospores as previously described (Desoignies et al. 2011). Ten thousand BNYVV-transmitting and virus-free zoospores were inoculated to three-week-old *B. vulgaris* KWS2320 roots. Negative controls were mock-inoculated with zoospore-free solutions produced with mock-inoculated *B. macrocarpa* plants following exactly the same procedure, to maintain uniform conditions between treatments. The general scheme of viruliferous inoculum production is represented in Figure 7.

Experimental design. Three bioassays comprising three treatments—mock-inoculated sugar beet, sugar beet infected with *P. betae* alone, and sugar beet infected with *P. betae* together with BNYVV—were conducted. Each bioassay was performed in two successive phases (Fig. 7). In the first phase, *P. betae* zoospores inoculum carrying or without BNYVV were produced on *B. macrocarpa* plantlets (19, 15, and 33 plants in bioassays 1, 2, and 3, respectively). This plant species was used for its ability to be systemically infected and to multiply BNYVV. In the second phase, susceptible *B. vulgaris* plantlets from strain KWS2320 were inoculated with *P. betae* zoospores, carrying or not the virus, produced in the first phase. In both first bioassays, 30 plants were inoculated with viruliferous zoospores, 20 plants with virus-free zoospores, and 10 plants were mock-inoculated with a "fake" zoospore suspension produced from healthy *B. macrocarpa*. In the third bioassay, 80 plants (20 per timepoint, discussed below) were inoculated with viruliferous zoospores, 48 plants (12 per timepoint) with virus-free zoospores, and

24 plants (six per timepoint) were mock-inoculated. For the first two bioassays, the entire root systems of sugar beet plants were collected at 28 dpi, were briefly washed in autoclaved water, were quickly snap-frozen, fully homogenized in liquid nitrogen, using a mortar and pestle, and were stored at −80°C until processed. In the third bioassay, roots were collected after 24 h, and 7, 14, and 28 days. At 14 and 28 dpi, two small portions (5 mm of taproot and all lateral roots attached) of each root system were excised for microscope observation. The rest was snap-frozen and ground in liquid nitrogen with a mortar and pestle and was stored at −80°C, as were the complete root systems collected at 1 and 7 dpi.

Nucleic acids extractions and RT-PCR.

For every sample, 30 to 50 mg of root powder were homogenized, using FastPrep (MP Biomedicals, Santa Ana, CA, U.S.A.) for 40 s at 6 m s^{-1}, and were used for total RNA extraction using Trizol reagent (Invitrogen, Waltham, MA, U.S.A.) according to the manufacturer instructions. RNA samples from *B. vulgaris* were then treated with RQ1 RNase-free DNase

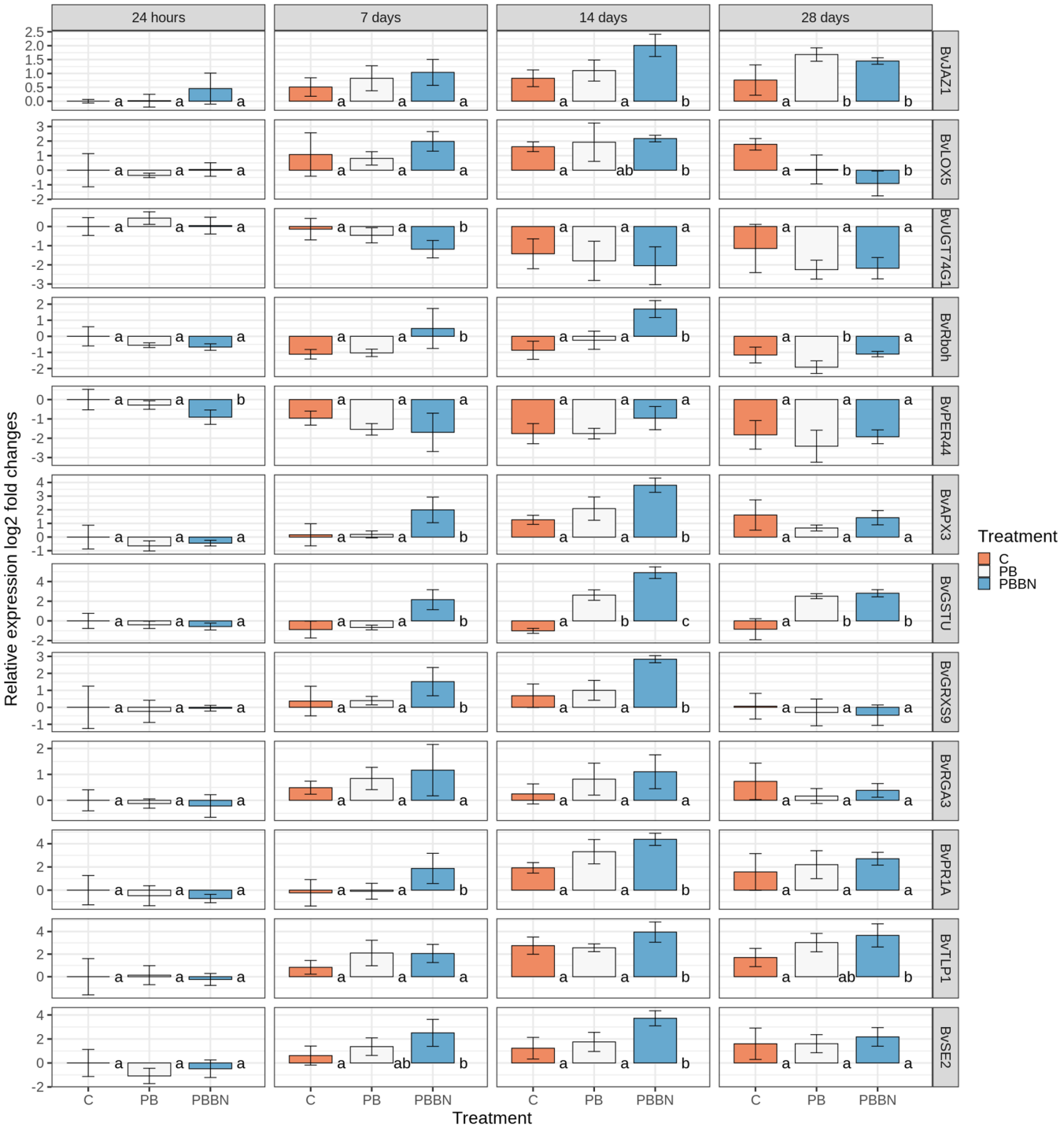

Fig. 6. Reverse transcription quantitative PCR expression of five genes related to oxidative stress regulation (*BvRboh*, *BvPER44*, *BvAPX3*, *BvGSTU8*, *BvGRXS9*) and seven plant defense genes (*BvRGA3*, *BvPR1A*, *BvTLP1*, *BvSE2*, *BvJAZ1*, *BvLOX5*, *BvUGT74G1*) at 1, 7, 14, and 28 days postinoculation. Data represent the means ± standard deviation and significantly different levels for each gene at each timepoint are indicated by different lower-case letters. C = mock-inoculated plants, PB = plants infected with *Polymyxa betae* alone, and PBBN = plants infected with *P. betae* and the beet necrotic yellow vein virus (BNYVV).

(Promega, Madison, WI, U.S.A.), were further purified with a phenol/chlorophorm/isoamyl alcohol (124:25:1) solution, and were kept in RNAse-free water at −80°C until needed. In the third bioassay, 50 mg of root powder was also used for DNA extraction at each timepoint, following a cetyltrimethylammonium bromide extraction procedure (Brandfass and Karlovsky 2008) after homogenization in FastPrep for 40 s at 6 m s^{-1}. The presence of *P. betae* and BNYVV in inoculated plants was then verified using the multiplex reverse transcriptase PCR (Meunier et al. 2003), and BNYVV infection was confirmed using simplex RT-PCR targeting each of the four BNYVV RNAs in the first two assays and RNA2 in the third one (a list of primers is available in Supplementary Table S9). All RT-PCRs were performed using M-MLV reverse transcriptase as described by Desoignies et al. (2014) and GoTaq G2 DNA polymerase (Promega) using manufacturer instructions. The amplification reaction for simplex RT-PCR comprised a first denaturation step at 95°C for 3 min, and then, 35 cycles of 30 s at 95°C, 30 s at 60°C, and 30 s at 72°C, and a final elongation step of 7 min at 72°C.

RNA-sequencing.

RNA quantity and purity were evaluated using a NanoDrop 1000 spectrophotometer and quality was visually evaluated after electrophoresis on a denaturant RNA gel (0.65% formaldehyde, 1.2% agarose). Five (mock-inoculated and *P. betae* alone) or six (*P. betae* together with BNYVV) biological replicates were selected for RNA sequencing from the first bioassay (28 dpi) based on RNA quantity and integrity as well as on the detection of required inoculum components (*P. betae*, BNYVV RNAs 1, 2, 3, and 4). For each sample, 800 ng of RNA suspended in 25 µl of RNAse-free water was sent to Fasteris SA (Geneva, Switzerland), which performed additional quantity and integrity assessments, polyA selection and library preparation with the TruSeq Stranded mRNA Library Prep kit (Illumina, San Diego, CA, U.S.A.), and paired-end sequencing (2 × 100 bp) on a Novaseq 6000 platform (Illumina). Data analysis was performed in-house.

Bioinformatics.

Fastq files containing paired raw reads were received from Fasteris. An initial quality check was performed with FastQC v.0.72 (Andrews 2010). Illumina adapters (ILLUMINACLIP: TruSeq3) and quality trimming (sliding window 4bp; average quality score > 20) was achieved using Trimmomatic v0.36.5 (Bolger et al. 2014). Reads shorter than 20 nucleotides were removed. Poly-G tails contaminations with a minimum length of 10, commonly seen in NovaSeq/NextSeq data, were trimmed with Fastp v.0.19.5 (Chen et al. 2018). The FastQC check was repeated to confirm improvement.

RNA-seq data were aligned to the *P. betae* reference genome (accession number ERZ3364346) using STAR v.2.7.3a in two-pass mode (Dobin et al. 2013) with the following non-default parameters: intron sizes were set to 15 minimum and 500 maximum, alignments with a ratio of mismatches to read length of maximum 0.04 were considered, minimum overhang for novel spliced alignments and annotated spliced alignments were set to 8 and 1, respectively, maximum number of loci a read is allowed to map was set to 20, maximum allowed gap between two mates was 2,000. Unmapped reads were then aligned to the *Beta vulgaris* reference genome (Dohm et al. 2014) (RefSeq assembly accession GCF_000511025.2), with the same settings except that intron sizes were adjusted to a minimum of 20 and a maximum of 5,000, allowing the gap between two mates to be adjusted to a maximum of 5,000. Since current *P. betae* genome annotations greatly rely on *in silico* gene predictions with limited transcriptomic support, *P. betae* transcripts were assembled using StringTie with default settings, except for the strand information specified to "reverse (RF)" (Pertea et al. 2015). All assembled transcripts were then merged with StringTie merge mode and were aggregated with the available annotation

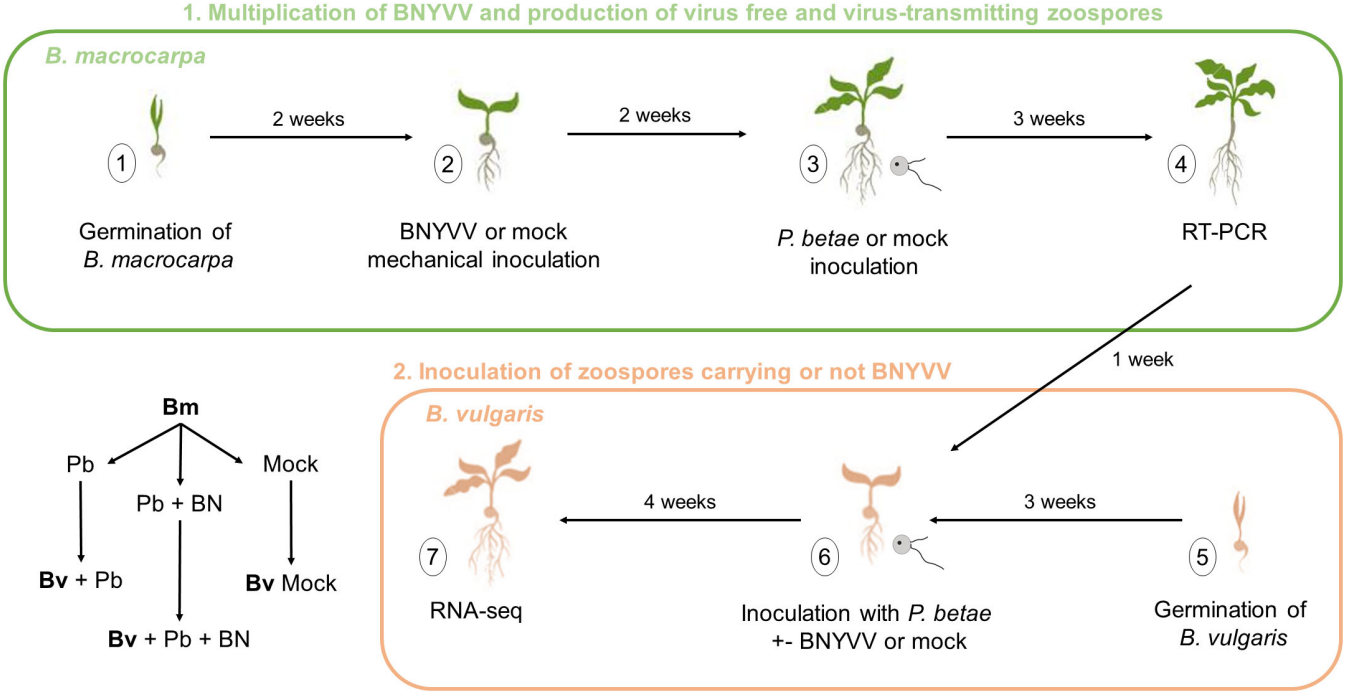

Fig. 7. Schematic representation of the seven successive steps of the bioassay performed to produce sugar beets infected with *Polymyxa betae* and beet necrotic yellow vein virus (BNYVV) from virus-free zoospores of the vector and BNYVV inoculum (infected sap of *Beta macrocarpa* symptomatic leaves), including virus-transmitting zoospore production on *B. macrocarpa* (1 to 4, upper part) and their inoculation on *Beta vulgaris* (5 to 7, bottom part). Timing is shown on arrows. A summary diagram is shown at the bottom left. Bm = *B. macrocarpa*, Bv = *B. vulgaris*, Pb = *P. betae*, BN = BNYVV, Mock = inoculum produced and inoculated with the same method but in absence of one or both Pb and BN.

(Decroës et al. 2022) using GffCompare (Pertea and Pertea 2020), with default settings. Read counts on both genomes' features were then computed with Htseq-count v.0.9.1 with the "union" mode and the strandedness option set to "reverse" (Anders et al. 2015). Open reading frames (ORFs) were predicted on *P. betae* assembled transcripts using TransDecoder v3.0.1 (B. Haas and A. Papanicolaou, available online). The single best ORF on each transcript was retained, prioritizing homology searches (BlastP against SWISS-PROT; hmmscan against Pfam) and ORF length. Translated peptide sequences were then annotated with Trinotate v3.2.2 (Bryant et al. 2017). Differential gene expression analysis was performed using the R software with edgeR v3.28.1 and limma v3.42.2 R/Bioconductor packages as described by Law et al. (2018). Notably, lowly expressed gene filtering and normalization with the trimmed mean of M-values method were achieved using "filterByExpr" and "calcNormFactors" functions in edgeR, respectively. Linear models (Smyth 2004) combined with abundance-dependent and sample-level weights (Law et al. 2014; Liu et al. 2015b) were fitted to the data using the limma package with the "voomWithQualityWeights" function. The choice of this strategy was based on the fact that multidimensional scaling plots showed some variability between replicates (Liu et al. 2015a). DEGs of *B. vulgaris* were determined from *P* values computed from empirical Bayes moderated *t* statistics, using the "treat" method (McCarthy and Smyth 2009) with a fold change (FC) of 1.2. DEGs of *P. betae* were determined using an adjusted *P* value cutoff of 0.05 without FC requirement. Plant genes were further annotated with Mercator4, and DEGs were classified in functional context (e.g., pathways) within MapMan4 (Schwacke et al. 2019) and the KEGG *B. vulgaris* (Kanehisa et al. 2017) frameworks. RGAs were classified according to Dohm et al. (2014). PR-like genes were searched in *B. vulgaris* refseq-rna, using tBLASTn (E value < 1e-05) with PR family founder proteins, coding as queries and manually refined, based on the reference *B. vulgaris* annotation. The expression of selected gene groups was represented on heatmaps with the pheatmap v1.0.12 R package. Other data were visualized with the ggplot2 v3.3.2 R package.

P. betae microscopic observation.

Root samples from the third bioassay were used to assess *P. betae* structure abundances at 14 and 28 dpi. To this end, 10 pieces of roots (approximately 5 mm long) were randomly selected from two portions of each root system. These portions were located at a midpoint of the taproot (called the "middle" part) and at 1 cm below the collar (called the "upper" part). The abundances of *P. betae* plasmodia, sporangia, and sporosori were visually assessed in each root portion after cotton blue lactophenol staining as described by Legrève et al. (1998), but using a customized semiquantitative 0 to 5 scale, where 0 = no infection, 1 = <10% cells infected by a particular development stage, 2 = 10 to 30% cells infected, 3 = 30 to 50% cells infected, 4 = 50 to 70% cells infected, 5 = >70% cells infected. Then, an infection index was calculated for each plant in the upper and middle part of the roots using the following formulae: $\Sigma_{i=0}{}^{5}(ni * i)/\Sigma_{i=0}{}^{5}ni$, where ni is the number of rootlets at infection level i (from 0 to 5).

Four weeks after inoculation, five root pieces were randomly selected from the middle part of the root system and were vacuum infiltrated with the LD540 lipophilic dye (Spandl et al. 2009) as described by Jurkiewicz et al. (2018). Roots were immediately imaged in confocal microscopy with a pinhole of 1 airy unit (excitation 488 nm; Zeiss LSM 710, Zeiss, Thornwood, NY, U.S.A.). Each image was captured using the same settings, in order to allow comparison of LD-derived fluorescence in the presence or the absence of BNYVV. LD fluorescence was quantified in 10 optical fields distributed in five root pieces per sample, using the ZEN 2 (blue edition) image analysis software (Carl Zeiss AG, Oberkochen, Germany).

RT-qPCR analysis.

In two bioassays, RT-qPCR analyses were carried out to quantify the proportion of *P. betae ITS1* transcripts in comparison with the expression of *B. vulgaris 18S* gene after 28 days (primers are listed in Supplementary Table S8). A qPCR targeting DNA template of the same genes was achieved in a third bioassay at four timepoints (1, 7, 14, and 21 days after inoculation). The relative gene expression quantification of 12 genes of interest and two reference genes was also achieved in this third assay. Moreover, the relative gene expression quantification of 10 genes of interest and two reference genes was also achieved on RNA extract used in the RNA-seq analysis in order to confirm RNA-seq results. The list of targeted genes and primers is available in Supplementary Table S9. When needed, cDNA was synthesized from 2 to 3 μg of Dnase-treated RNA, using M-MLV reverse transcriptase (Promega) and anchored oligo$(dT)_{18}$ primers or the corresponding reverse primer for *ITS* and *18S* amplifications. qPCR assays were carried out using Takyon No ROX SYBR 2X MasterMix blue dTTP (Eurogentec, Seraing, Belgium) on a CFX96 real-time system (Bio-Rad, Hercules, CA, U.S.A.). For each sample, a reaction was set up, with 10 μl of MasterMix, 0.5 μl of each primer (20 μM), 7 μl of diethyl pyrocarbonate–treated water and 2 μl of cDNA, using the following protocol: denaturation step at 95 C for 7 min, then, 40 cycles of 30 s at 95°C, 30 s at 60°C, and 30 s at 72°C, and a final melting curve (55 to 9 °C with a heating rate of 0.5°C per second). Each qPCR assay was performed in two replicates. Reaction efficiency in each plate was monitored through the establishment of standard curves, using five serial dilution of target cDNAs in order to guarantee the linearity of amplification over the samples quantification cycle range. Only qPCR whose efficiency comprised 90 to 105% were considered. Data analysis was performed using CFX Manager software (Bio-Rad) and the R software using the $2^{-\Delta\Delta Ct}$ method (Livak and Schmittgen 2001) and considering the MIQE recommendations (Bustin et al. 2009). Significantly different levels were determined at each timepoint by *t* test, applying a Bonferroni correction for multiple testing.

Conclusions.

A soil-free BNYVV transmission protocol was successfully applied to achieve a transcriptomic analysis of the tripartite interaction between *P. betae*, BNYVV, and the sugar beet, revealing that multiple pathways are involved. When inoculated alone, *P. betae* attenuated the defense response of sugar beet, as shown by the downregulation of defense-related genes belonging to RGA, TF, and cell-wall peroxidase families and the upregulation of genes involved in redox homeostasis, such as *GSTs*. This could be associated with the absence of symptoms and suggests that the interaction between the plant and the protist can be described as commensalism (Bjorbækmo et al. 2020). The regulation of plant genes involved with lipid metabolism, such as FA synthase genes, were also observed during resting spore formation and could be related to the production of numerous LD observed in *P. betae* structures. After inoculation with viruliferous zoospores, BNYVV hastened the primary invasion of *B. vulgaris* roots by *P. betae*, between 1 and 14 dpi. This faster early multiplication of *P. betae* could be related to the regulation of genes related to plant cell-wall integrity, not to mention the effect of BNYYV suppressors of RNA silencing on the plant, also beneficial for the protist. The upregulation of plant genes related to defense signaling pathways as well as PR proteins and phenolic compounds synthesis was also observed. The induction of plant defenses was correlated with a quicker induction of the resting spore stage of the protist.

These results will help in deciphering the highly dynamic interaction between the three different partners at different stages of the infection process, as indicated by expression changes already noticed. It provides an additional example of how a virus, BNYYV, is able to manipulate its host plant, sugar beet, and its vector, *Polymyxa betae*, to improve its transmission, thus ensuring its survival, as already shown for insect-transmitted plant viruses (Blanc and Michalakis 2016; Ziegler-Graff 2020).

Data availability.

Illumina raw reads are deposited at the European Nucleotide Archive (ENA) under accession numbers ERR7334425 to ERR7334440 in BioProject PRJEB48689.

ACKNOWLEDGMENTS

We thank C. Thiele (Max Planck Institute of Molecular Cell Biology and Genetics, Dresden, Germany) for generously providing LD540 dye, H. Batoko for valuable advice, and E. Mutasa-Gottgens for proofreading the paper. We also express our gratitude to B. Schulz (KWS SAAT SE, Einbeck, Germany) for kindly providing seeds from the KWS2320 sugar beet.

AUTHOR-RECOMMENDED INTERNET RESOURCE

TransDecoder: transdecoder.github.io

LITERATURE CITED

Agarwal, A., Kaul, V., Faggian, R., Rookes, J. E., Ludwig-Müller, J., and Cahill, D. M. 2011. Analysis of global host gene expression during the primary phase of the *Arabidopsis thaliana–Plasmodiophora brassicae* interaction. Funct. Plant Biol. 38:462-478.

Anders, S., Pyl, P. T., and Huber, W. 2015. HTSeq—A Python framework to work with high-throughput sequencing data. Bioinformatics 31:166-169.

Andrews, S. 2010. FastQC: A quality control tool for high throughput sequence data. Babraham Bioinformatics, Babraham Institute, Cambridge, U.K.

Bagayoko, I., Celli, M. G., Romay, G., Poulicard, N., Pinel-Galzi, A., Julian, C., Filloux, D., Roumagnac, P., Sérémé, D., Bragard, C., and Hébrard, E. 2021. Genetic diversity of *Rice stripe necrosis virus* and new insights into evolution of the genus *Benyvirus*. Viruses 13:737.

Barbez, E., Kubeš, M., Rolčík, J., Béziat, C., Pěnčík, A., Wang, B., Rosquete, M. R., Zhu, J., Dobrev, P. I., Lee, Y., Zažímalovà, E., Petrášek, J., Geisler, M., Friml, J., and Kleine-Vehn, J. 2012. A novel putative auxin carrier family regulates intracellular auxin homeostasis in plants. Nature 485:119-122.

Barr, D. J. S., and Allan, P. M. E. 1982. Zoospore ultrastructure of *Polymyxa graminis* (Plasmodiophoromycetes). Can. J. Bot. 60:2496-2504.

Barr, K. J., and Asher, M. J. C. 1996. Studies on the life-cycle of *Polymyxa betae* in sugar beet roots. Mycol. Res. 100:203-208.

Benjamins, R., Quint, A., Weijers, D., Hooykaas, P., and Offringa, R. 2001. The PINOID protein kinase regulates organ development in *Arabidopsis* by enhancing polar auxin transport. Dev. Camb. Engl. 128:4057-4067.

Bi, K., He, Z., Gao, Z., Zhao, Y., Fu, Y., Cheng, J., Xie, J., Jiang, D., and Chen, T. 2016. Integrated omics study of lipid droplets from *Plasmodiophora brassicae*. Sci. Rep. 6:36965.

Bjorbækmo, M. F. M., Evenstad, A., Røsæg, L. L., Krabberød, A. K., and Logares, R. 2020. The planktonic protist interactome: Where do we stand after a century of research? ISME J. 14:544-559.

Blanc, S., and Michalakis, Y. 2016. Manipulation of hosts and vectors by plant viruses and impact of the environment. Curr. Opin. Insect Sci. 16: 36-43.

Bol, J. F., Linthorst, H. J. M., and Cornelissen, B. J. C. 1990. Plant pathogenesis-related proteins induced by virus infection. Annu. Rev. Phytopathol. 28:113-138.

Bolger, A. M., Lohse, M., and Usadel, B. 2014. Trimmomatic: A flexible trimmer for Illumina sequence data. Bioinformatics 30:2114-2120.

Brandfass, C., and Karlovsky, P. 2008. Upscaled CTAB-based DNA extraction and real-time PCR assays for *Fusarium culmorum* and *F. graminearum* DNA in plant material with reduced sampling error. Int. J. Mol. Sci. 9:2306-2321.

Bryant, D. M., Johnson, K., DiTommaso, T., Tickle, T., Couger, M. B., Payzin-Dogru, D., Lee, T. J., Leigh, N. D., Kuo, T.-H., Davis, F. G., Bateman, J., Bryant, S., Guzikowski, A. R., Tsai, S. L., Coyne, S., Ye, W. W., Freeman, R. M., Peshkin, L., Tabin, C. J., Regev, A., Haas, B. J., and Whited, J. L. 2017. A tissue-mapped axolotl de novo transcriptome enables identification of limb regeneration factors. Cell Rep. 18: 762-776.

Bulman, S., Richter, F., Marschollek, S., Benade, F., Jülke, S., and Ludwig-Müller, J. 2018. *Arabidopsis thaliana* expressing PbBSMT, a gene encoding a SABATH-type methyltransferase from the plant pathogenic protist *Plasmodiophora brassicae*, show leaf chlorosis and altered host susceptibility. Plant Biol. Stuttg. 21:120-130.

Burketová, L., Štillerová, K., and Feltlová, M. 2003. Immunohistological localization of chitinase and β-1,3-glucanase in rhizomania-diseased and benzothiadiazole treated sugar beet roots. Physiol. Mol. Plant Pathol. 63:47-54.

Bustin, S. A., Benes, V., Garson, J. A., Hellemans, J., Huggett, J., Kubista, M., Mueller, R., Nolan, T., Pfaffl, M. W., Shipley, G. L., Vandesompele, J., and Wittwer, C. T. 2009. The MIQE guidelines: Minimum information for publication of quantitative real-time PCR experiments. Clin. Chem. 55:611-622.

Castilleux, R., Plancot, B., Gügi, B., Attard, A., Loutelier-Bourhis, C., Lefranc, B., Nguema-Ona, E., Arkoun, M., Yvin, J.-C., Driouich, A., and Vicré, M. 2020. Extensin arabinosylation is involved in root response to elicitors and limits oomycete colonization. Ann. Bot. 125: 751-763.

Chen, S., Zhou, Y., Chen, Y., and Gu, J. 2018. fastp: An ultra-fast all-in-one FASTQ preprocessor. Bioinformatics 34:i884-i890.

Chen, W., Li, Y., Yan, R., Ren, L., Liu, F., Zeng, L., Sun, S., Yang, H., Chen, K., Xu, L., Liu, L., Fang, X., and Liu, S. 2021. SnRK1.1-mediated resistance of *Arabidopsis thaliana* to clubroot disease is inhibited by the novel *Plasmodiophora brassicae* effector PBZF1. Mol. Plant Pathol. 22:1057-1069.

Chen, W., Li, Y., Yan, R., Xu, L., Ren, L., Liu, F., Zeng, L., Yang, H., Chi, P., Wang, X., Chen, K., Ma, D., and Fang, X. 2019. Identification and characterization of *Plasmodiophora brassicae* primary infection effector candidates that suppress or induce cell death in host and nonhost plants. Phytopathology 109:1689-1697.

Chiba, S., Hleibieh, K., Delbianco, A., Klein, E., Ratti, C., Ziegler-Graff, V., Bouzoubaa, S., and Gilmer, D. 2013. The *Benyvirus* RNA silencing suppressor is essential for long-distance movement, requires both zinc-finger and nols basic residues but not a nucleolar localization for its silencing-suppression activity. Mol. Plant-Microbe Interact. 26:168-181.

Cosgrove, D. J. 2015. Plant expansins: Diversity and interactions with plant cell walls. Curr. Opin. Plant Biol. 25:162-172.

Crutzen, F., Mehrvar, M., Gilmer, D., and Bragard, C. 2009. A full-length infectious clone of beet soil-borne virus indicates the dispensability of the RNA-2 for virus survival in planta and symptom expression on *Chenopodium quinoa* leaves. J. Gen. Virol. 90:3051-3056.

D'Ambra, V., and Mutto, S. 1977. The ultrastructure of *Polymyxa betae* zoospore exit-tube differentiation. Can. J. Bot. 55:831-839.

Dao, T. T. H., Linthorst, H. J. M., and Verpoorte, R. 2011. Chalcone synthase and its functions in plant resistance. Phytochem. Rev. 10:397.

Decroës, A., Calusinska, M., Delfosse, P., Bragard, C., and Legrève, A. 2019. First draft genome sequence of a *Polymyxa* genus member, *Polymyxa betae*, the protist vector of rhizomania. Microbiol. Resour. Announc. 8:e01509-18.

Decroës, A., Li, J.-M., Richardson, L., Mutasa-Gottgens, E., Lima-Mendez, G., Mahillon, M., Bragard, C., Finn, R. D., and Legrève, A. 2022. Metagenomics approach for *Polymyxa betae* genome assembly enables comparative analysis towards deciphering the intracellular parasitic lifestyle of the plasmodiophorids. Genomics 114:9-22.

Deng, Y., Dong, H., Mu, J., Ren, B., Zheng, B., Ji, Z., Yang, W.-C., Liang, Y., and Zuo, J. 2010. *Arabidopsis* histidine kinase CKI1 acts upstream of histidine phosphotransfer proteins to regulate female gametophyte development and vegetative growth. Plant Cell 22:1232-1248.

Desoignies, N., Carbonell, J., Moreau, J.-S., Conesa, A., Dopazo, J., and Legrève, A. 2014. Molecular interactions between sugar beet and *Polymyxa betae* during its life cycle. Ann. Appl. Biol. 164:244-256.

Desoignies, N., Stocco, C., Bragard, C., and Legrève, A. 2011. A new phenotype of *Polymyxa betae* in *Arabidopsis thaliana*. Eur. J. Plant Pathol. 131:27-38.

Devos, S., Laukens, K., Deckers, P., Van Der Straeten, D., Beeckman, T., Inzé, D., Van Onckelen, H., Witters, E., and Prinsen, E. 2006. A hormone and proteome approach to picturing the initial metabolic events during *Plasmodiophora brassicae* infection on *Arabidopsis*. Mol. Plant-Microbe Interact. 19:1431-1443.

Dieryck, B., Otto, G., Doucet, D., Legrève, A., Delfosse, P., and Bragard, C. 2009. Seed, soil and vegetative transmission contribute to the spread of pecluviruses in Western Africa and the Indian sub-continent. Virus Res. 141:184-189.

Dieryck, B., Weyns, J., Doucet, D., Bragard, C., and Legrève, A. 2011. Acquisition and transmission of *Peanut clump virus* by *Polymyxa graminis* on cereal species. Phytopathology 101:1149-1158.

Dimmer, E., Roden, L., Cai, D., Kingsnorth, C., and Mutasa-Göttgens, E. 2004. Transgenic analysis of sugar beet xyloglucan endotransglucosylase/hydrolase *Bv-XTH1* and *Bv-XTH2* promoters reveals overlapping tissue-specific and wound-inducible expression profiles. Plant Biotechnol. J. 2:127-139.

Dobin, A., Davis, C. A., Schlesinger, F., Drenkow, J., Zaleski, C., Jha, S., Batut, P., Chaisson, M., and Gingeras, T. R. 2013. STAR: Ultrafast universal RNA-seq aligner. Bioinformatics 29:15-21.

Dobisova, T., Hrdinova, V., Cuesta, C., Michlickova, S., Urbankova, I., Hejatkova, R., Zadnikova, P., Pernisova, M., Benkova, E., and Hejatko, J. 2017. Light controls cytokinin signaling via transcriptional regulation of constitutively active sensor histidine kinase CKI1. Plant Physiol. 174:387-404.

Dohm, J. C., Minoche, A. E., Holtgräwe, D., Capella-Gutiérrez, S., Zakrzewski, F., Tafer, H., Rupp, O., Sörensen, T. R., Stracke, R., Reinhardt, R., Goesmann, A., Kraft, T., Schulz, B., Stadler, P. F., Schmidt, T., Gabaldón, T., Lehrach, H., Weisshaar, B., and Himmelbauer, H. 2014. The genome of the recently domesticated crop plant sugar beet (*Beta vulgaris*). Nature 505:546-549.

Fan, H., Sun, H., Wang, Y., Zhang, Y., Wang, X., Li, D., Yu, J., and Han, C. 2014. Deep sequencing–based transcriptome profiling reveals comprehensive insights into the responses of *Nicotiana benthamiana* to *Beet necrotic yellow vein virus* infections containing or lacking RNA4. PLoS One 9:e85284.

Fan, H., Zhang, Y., Sun, H., Liu, J., Wang, Y., Wang, X., Li, D., Yu, J., and Han, C. 2015a. Transcriptome analysis of beta macrocarpa and identification of differentially expressed transcripts in response to *Beet necrotic yellow vein virus* infection. PLoS One 10:e0132277.

Fan, J., Ning, K., Zeng, X., Luo, Y., Wang, D., Hu, J., Li, J., Xu, H., Huang, J., Wan, M., Wang, W., Zhang, D., Shen, G., Run, C., Liao, J., Fang, L., Huang, S., Jing, X., Su, X., Wang, A., Bai, L., Hu, Z., Xu, J., and Li, Y. 2015b. Genomic foundation of starch-to-lipid switch in oleaginous *Chlorella* spp. Plant Physiol. 169:2444-2461.

Fei, W., Feng, J., Rong, S., Strelkov, S. E., Gao, Z., and Hwang, S.-F. 2015. Infection and gene expression of the clubroot pathogen *Plasmodiophora brassicae* in resistant and susceptible canola cultivars. Plant Dis. 100: 824-828.

Fernando Gil, J., Liebe, S., Thiel, H., Lennefors, B.-L., Kraft, T., Gilmer, D., Maiss, E., Varrelmann, M., and Savenkov, E. I. 2018. Massive upregulation of LBD transcription factors and EXPANSINs highlights the regulatory programs of rhizomania disease. Mol. Plant Pathol. 19: 2333-2348.

Fernando Gil, J., Wibberg, D., Eini, O., Savenkov, E. I., Varrelmann, M., and Liebe, S. 2020. Comparative transcriptome analysis provides molecular insights into the interaction of *Beet necrotic yellow vein virus* and *Beet soil-borne mosaic virus* with their host sugar beet. Viruses 12:76.

Flobinus, A., Chevigny, N., Charley, P. A., Seissler, T., Klein, E., Bleykasten-Grosshans, C., Ratti, C., Bouzoubaa, S., Wilusz, J., and Gilmer, D. 2018. Beet necrotic yellow vein virus noncoding RNA production depends on a 5′→3′ xrn exoribonuclease activity. Viruses 10:137.

Flobinus, A., Hleibieh, K., Klein, E., Ratti, C., Bouzoubaa, S., and Gilmer, D. 2016. A viral noncoding RNA complements a weakened viral RNA silencing suppressor and promotes efficient systemic host infection. Viruses 8:272.

Foley, R. C., and Singh, K. B. 2004. TGA5 acts as a positive and TGA4 acts as a negative regulator of ocs element activity in Arabidopsis roots in response to defence signals. FEBS Lett. 563:141-145.

Forouhar, F., Yang, Y., Kumar, D., Chen, Y., Fridman, E., Park, S. W., Chiang, Y., Acton, T. B., Montelione, G. T., Pichersky, E., Klessig, D. F., and Tong, L. 2005. Structural and biochemical studies identify tobacco SABP2 as a methyl salicylate esterase and implicate it in plant innate immunity. Proc. Natl. Acad. Sci. U.S.A. 102:1773-1778.

Galindo-González, L., Hwang, S.-F., and Strelkov, S. E. 2021. Candidate effectors of *Plasmodiophora brassicae* pathotype 5× during infection of two *Brassica napus* genotypes. Front. Microbiol. 12:3325.

Gerik, J. S., and Duffus, J. E. 1988. Differences in vectoring ability and aggressiveness of isolates of *Polymyxa betae*. Phytopathology 78: 1340-1343.

Gilmer, D., and Ratti, C. 2017. ICTV virus taxonomy profile: *Benyviridae*. J. Gen. Virol. 98:1571-1572.

Gullner, G., Komives, T., Király, L., and Schröder, P. 2018. Glutathione S-transferase enzymes in plant-pathogen interactions. Front. Plant Sci. 9.

Han, J.-H., Shin, J.-H., Lee, Y.-H., and Kim, K. S. 2018. Distinct roles of the *YPEL* gene family in development and pathogenicity in the ascomycete fungus *Magnaporthe oryzae*. Sci. Rep. 8:14461.

Haudecoeur, R., Ahmed-Belkacem, A., Yi, W., Fortuné, A., Brillet, R., Belle, C., Nicolle, E., Pallier, C., Pawlotsky, J.-M., and Boumendjel, A. 2011. Discovery of naturally occurring aurones that are potent allosteric inhibitors of hepatitis c virus RNA-dependent RNA polymerase. J. Med. Chem. 54:5395-5402.

Heidel, G. B., Rush, C. M., Kendall, T. L., Lommel, S. A., and French, R. C. 1997. Characteristics of *Beet soilborne mosaic virus*, a furo-like virus infecting sugar beet. Plant Dis. 81:1070-1076.

Hoagland, D. R., and Arnon, D. I. 1950. The water-culture method for growing plants without soil. Circ. Calif. Agric. Exp. Stn. 347:32.

Hossain, M. M., Pérez-López, E., Todd, C. D., Wei, Y., and Bonham-Smith, P. C. 2021. Endomembrane-targeting *Plasmodiophora brassicae* effectors modulate PAMP triggered immune responses in plants. Front. Microbiol. 12:651279.

Irani, S., Todd, C. D., Wei, Y., and Bonham-Smith, P. C. 2019. Changes in phenylpropanoid pathway gene expression in roots and leaves of susceptible and resistant Brassica napus lines in response to *Plasmodiophora brassicae* inoculation. Physiol. Mol. Plant Pathol. 106:196-203.

Irani, S., Trost, B., Waldner, M., Nayidu, N., Tu, J., Kusalik, A. J., Todd, C. D., Wei, Y., and Bonham-Smith, P. C. 2018. Transcriptome analysis of response to *Plasmodiophora brassicae* infection in the *Arabidopsis* shoot and root. BMC Genomics 19:23.

Jashni, M. K., Mehrabi, R., Collemare, J., Mesarich, C. H., and de Wit, P. J. G. M. 2015. The battle in the apoplast: Further insights into the roles of proteases and their inhibitors in plant-pathogen interactions. Front. Plant Sci. 6:584.

Jia, H., Wei, X., Yang, Y., Yuan, Y., Wei, F., Zhao, Y., Yang, S., Yao, Q., Wang, Z., Tian, B., and Zhang, X. 2017. Root RNA-seq analysis reveals a distinct transcriptome landscape between clubroot-susceptible and clubroot-resistant Chinese cabbage lines after *Plasmodiophora brassicae* infection. Plant Soil 421:93-105.

Jones, R. a. C., and Harrison, B. D. 1969. The behaviour of potato mop-top virus in soil, and evidence for its transmission by *Spongospora subterranea* (Wallr.) Lagerh. Ann. Appl. Biol. 63:1-17.

Jurkiewicz, P., Melser, S., Maucourt, M., Ayeb, H., Veljanovski, V., Maneta-Peyret, L., Hooks, M., Rolin, D., Moreau, P., and Batoko, H. 2018. The multistress-induced Translocator protein (TSPO) differentially modulates storage lipids metabolism in seeds and seedlings. Plant J. 96:274-286.

Kalunke, R. M., Tundo, S., Benedetti, M., Cervone, F., De Lorenzo, G., and D'Ovidio, R. 2015. An update on polygalacturonase-inhibiting protein (PGIP), a leucine-rich repeat protein that protects crop plants against pathogens. Front. Plant Sci. 6:146.

Kanehisa, M., Furumichi, M., Tanabe, M., Sato, Y., and Morishima, K. 2017. KEGG: New perspectives on genomes, pathways, diseases and drugs. Nucleic Acids Res. 45:D353-D361.

Kanyuka, K., Ward, E., and Adams, M. J. 2003. *Polymyxa graminis* and the cereal viruses it transmits: A research challenge. Mol. Plant Pathol. 4:393-406.

Koenig, R., and Stein, B. 1990. Distribution of beet necrotic yellow vein virus in mechanically inoculated sugarbeet plantlets of cultivars with different degrees of rizomania resistance. Pages 87-90 in: Proc. First Symp. Int. Work. Group Plant Viruses Fungal Vectors, 1st, Stuttgart, Germany.

Kohorn, B., and Kohorn, S. 2012. The cell wall-associated kinases, WAKs, as pectin receptors. Front. Plant Sci. 3:88.

Larson, R. L., Wintermantel, W. M., Hill, A., Fortis, L., and Nunez, A. 2008. Proteome changes in sugar beet in response to *Beet necrotic yellow vein virus*. Physiol. Mol. Plant Pathol. 72:62-72.

Law, C. W., Alhamdoosh, M., Su, S., Dong, X., Tian, L., Smyth, G. K., and Ritchie, M. E. 2018. RNA-seq analysis is easy as 1-2-3 with limma, Glimma and edgeR. F1000Research 5:1408.

Law, C. W., Chen, Y., Shi, W., and Smyth, G. K. 2014. voom: Precision weights unlock linear model analysis tools for RNA-seq read counts. Genome Biol. 15:R29.

Lee, L., Telford, E. B., Batten, J. S., Scholthof, K.-B. G., and Rush, C. M. 2001. Complete nucleotide sequence and genome organization of *Beet soilborne mosaic virus*, a proposed member of the genus *Benyvirus*. Arch. Virol. 146:2443-2453.

Legrève, A., Delfosse, P., Vanpee, B., Goffin, A., and Maraite, H. 1998. Differences in temperature requirements between *Polymyxa* sp. of Indian origin and *Polymyxa graminis* and *Polymyxa betae* from temperate areas. Eur. J. Plant Pathol. 104:195-205.

Liu, J.-Y., Fan, H.-Y., Wang, Y., Zhang, Y.-L., Li, D.-W., Yu, J.-L., and Han, C.-G. 2017. Characterization of microRNAs of *Beta macrocarpa* and their responses to *Beet necrotic yellow vein virus* infection. PLoS One 12:e0186500.

Liu, R., Chen, K., Jansz, N., Blewitt, M. E., and Ritchie, M. E. 2015a. Transcriptional profiling of the epigenetic regulator Smchd1. Genom. Data 7:144-147.

Liu, R., Holik, A. Z., Su, S., Jansz, N., Chen, K., Leong, H. S., Blewitt, M. E., Asselin-Labat, M.-L., Smyth, G. K., and Ritchie, M. E. 2015b. Why weight? Modelling sample and observational level variability improves power in RNA-seq analyses. Nucleic Acids Res. 43:e97.

Livak, K. J., and Schmittgen, T. D. 2001. Analysis of relative gene expression data using real-time quantitative PCR and the $2^{-\Delta\Delta CT}$ method. Methods 25:402-408.

Lorenz, M. C., and Fink, G. R. 2002. Life and death in a macrophage: Role of the glyoxylate cycle in virulence. Eukaryot. Cell 1:657-662.

Ludwig-Müller, J., Jülke, S., Geiß, K., Richter, F., Mithöfer, A., Šola, I., Rusak, G., Keenan, S., and Bulman, S. 2015. A novel methyltransferase from the intracellular pathogen *Plasmodiophora brassicae* methylates salicylic acid: Salicylic acid methyltransferase from *P. brassicae*. Mol. Plant Pathol. 16:349-364.

Mahillon, M., Decroës, A., Peduzzi, C., Romay, G., Legrève, A., and Bragard, C. 2021. RNA silencing machinery contributes to inability of BSBV to establish infection in *Nicotiana benthamiana*: Evidence from characterization of agroinfectious clones of *Beet soil-borne virus*. J. Gen. Virol. 102:001530.

Malinowski, R., Truman, W., and Blicharz, S. 2019. Genius architect or clever thief—How *Plasmodiophora brassicae* reprograms host development to establish a pathogen-oriented physiological sink. Mol. Plant-Microbe Interact. 32:1259-1266.

McCarthy, D. J., and Smyth, G. K. 2009. Testing significance relative to a fold-change threshold is a TREAT. Bioinformatics 25:765-771.

McGrann, G. R. D., Grimmer, M. K., Mutasa-Göttgens, E. S., and Stevens, M. 2009. Progress towards the understanding and control of sugar beet rhizomania disease. Mol. Plant Pathol. 10:129-141.

McGrann, G. R. D., Martin, L. D., Kingsnorth, C. S., Asher, M. J. C., Adams, M. J., and Mutasa-Göttgens, E. S. 2007. Screening for genetic elements involved in the nonhost response of sugar beet to the plasmodiophorid cereal root parasite *Polymyxa graminis* by representational difference analysis. J. Gen. Plant Pathol. 73:260-265.

McGrann, G. R. D., Townsend, B. J., Antoniw, J. F., Asher, M. J. C., and Mutasa-Göttgens, E. S. 2009. Barley elicits a similar early basal defence response during host and non-host interactions with *Polymyxa* root parasites. Eur. J. Plant Pathol. 123:5-15.

Meunier, A., Schmit, J.-F., Stas, A., Kutluk, N., and Bragard, C. 2003. Multiplex reverse transcription-PCR for simultaneous detection of *Beet necrotic yellow vein virus*, *Beet soilborne virus*, and *Beet virus q* and their vector *Polymyxa betae* KESKIN on sugar beet. Appl. Environ. Microbiol. 69:2356-2360.

Mithen, R., and Magrath, R. 1992. A contribution to the life history of *Plasmodiophora brassicae*: Secondary plasmodia development in root galls of *Arabidopsis thaliana*. Mycol. Res. 96:877-885.

Murphy, D. J. 2012. The dynamic roles of intracellular lipid droplets: From archaea to mammals. Protoplasma 249:541-585.

Mutasa-Gottgens, E. S., Chwarszczynska, D. M., Halsey, K., and Asher, M. J. C. 2000. Specific polyclonal antibodies for the obligate plant parasite *Polymyxa*—A targeted recombinant DNA approach. Plant Pathol. 49: 276-287.

Nieberl, P., Ehrl, C., Pommerrenig, B., Graus, D., Marten, I., Jung, B., Ludewig, F., Koch, W., Harms, K., Flügge, U.-I., Neuhaus, H. E., Hedrich, R., and Sauer, N. 2017. Functional characterisation and cell specificity of BvSUT1, the transporter that loads sucrose into the phloem of sugar beet (*Beta vulgaris* L.) source leaves. Plant Biol. Stuttg. Ger. 19: 315-326.

Päsold, S., Siegel, I., Seidel, C., and Ludwig-Müller, J. 2010. Flavonoid accumulation in *Arabidopsis thaliana* root galls caused by the obligate biotrophic pathogen *Plasmodiophora brassicae*. Mol. Plant Pathol. 11:545-562.

Peltier, C., Schmidlin, L., Klein, E., Taconnat, L., Prinsen, E., Erhardt, M., Heintz, D., Weyens, G., Lefebvre, M., Renou, J.-P., and Gilmer, D. 2011. Expression of the *Beet necrotic yellow vein virus* p25 protein induces hormonal changes and a root branching phenotype in *Arabidopsis thaliana*. Transgenic Res. 20:443-466.

Pérez-López, E., Hossain, M. M., Tu, J., Waldner, M., Todd, C. D., Kusalik, A. J., Wei, Y., and Bonham-Smith, P. C. 2020. Transcriptome analysis identifies *Plasmodiophora brassicae* secondary infection effector candidates. J. Eukaryot. Microbiol. 67:337-351.

Pérez-López, E., Hossain, M. M., Wei, Y., Todd, C. D., and Bonham-Smith, P. C. 2021. A clubroot pathogen effector targets cruciferous cysteine proteases to suppress plant immunity. Virulence 12:2327-2340.

Pertea, G., and Pertea, M. 2020. GFF Utilities: GffRead and GffCompare. F1000Research 9:304.

Pertea, M., Pertea, G. M., Antonescu, C. M., Chang, T.-C., Mendell, J. T., and Salzberg, S. L. 2015. StringTie enables improved reconstruction of a transcriptome from RNA-seq reads. Nat. Biotechnol. 33:290-295.

Prillwitz, H., and Schlösser, E. 1992. Beet soil-borne virus: Occurrence, symptoms and effect on plant development. Meded. Van Fac. Landbouwwet. Univ. Gent. 57:295-302.

Quillet, L., Guilley, H., Jonard, G., and Richards, K. 1989. In vitro synthesis of biologically active beet necrotic yellow vein virus RNA. Virology 172:293-301.

Rahim, M. D., Andika, I. B., Han, C., Kondo, H., and Tamada, T. 2007. RNA4-encoded p31 of beet necrotic yellow vein virus is involved in efficient vector transmission, symptom severity and silencing suppression in roots. J. Gen. Virol. 88:1611-1619.

Reavy, B., Arif, M., Cowan, G. H., and Torrance, L. 1998. Association of sequences in the coat protein/readthrough domain of potato mop-top virus with transmission by *Spongospora subterranea*. J. Gen. Virol. 79: 2343-2347.

Schlösser, E. 1990. Rizomania. XII. Effect of BNYVV and BSBV on the development of *Polymyxa betae* Keskin. Rizomania XII Eff. BNYVV BSBV Dev. *Polymyxa betae* Keskin. 55:1069-1071.

Schmidlin, L., Bruyne, E. D., Weyens, G., Lefebvre, M., and Gilmer, D. 2008. Identification of differentially expressed root genes upon rhizomania disease. Mol. Plant Pathol. 9:741-751.

Schwacke, R., Ponce-Soto, G. Y., Krause, K., Bolger, A. M., Arsova, B., Hallab, A., Gruden, K., Stitt, M., Bolger, M. E., and Usadel, B. 2019. MapMan4: A refined protein classification and annotation framework applicable to multi-omics data analysis. Mol. Plant. 12:879-892.

Schwelm, A., Fogelqvist, J., Knaust, A., Jülke, S., Lilja, T., Bonilla-Rosso, G., Karlsson, M., Shevchenko, A., Dhandapani, V., Choi, S. R., Kim, H. G., Park, J. Y., Lim, Y. P., Ludwig-Müller, J., and Dixelius, C. 2015. The *Plasmodiophora brassicae* genome reveals insights in its life cycle and ancestry of chitin synthases. Sci. Rep. 5:11153.

Sergeeva, L. I., Keurentjes, J. J. B., Bentsink, L., Vonk, J., van der Plas, L. H. W., Koornneef, M., and Vreugdenhil, D. 2006. Vacuolar invertase regulates elongation of *Arabidopsis thaliana* roots as revealed by QTL and mutant analysis. Proc. Natl. Acad. Sci. U.S.A. 103:2994-2999.

Shrode, L. B., Lewis, Z. A., White, L. D., Bell-Pedersen, D., and Ebbole, D. J. 2001. *vvd* is required for light adaptation of conidiation-specific genes of *Neurospora crassa*, but not circadian conidiation. Fungal Genet. Biol. 32:169-181.

Siemens, J., González, M.-C., Wolf, S., Hofmann, C., Greiner, S., Du, Y., Rausch, T., Roitsch, T., and Ludwig-Müller, J. 2011. Extracellular invertase is involved in the regulation of clubroot disease in *Arabidopsis thaliana*. Mol. Plant Pathol. 12:247-262.

Siemens, J., Keller, I., Sarx, J., Kunz, S., Schuller, A., Nagel, W., Schmülling, T., Parniske, M., and Ludwig-Müller, J. 2006. Transcriptome analysis of *Arabidopsis* clubroots indicate a key role for cytokinins in disease development. Mol. Plant-Microbe Interact. 19:480-494.

Smyth, G. K. 2004. Linear models and empirical Bayes methods for assessing differential expression in microarray experiments. Stat. Appl. Genet. Mol. Biol. 3:1.

Spandl, J., White, D. J., Peychl, J., and Thiele, C. 2009. Live cell multicolor imaging of lipid droplets with a new dye, LD540. Traffic 10:1579-1584.

Tamada, T. 2016. General features of beet necrotic yellow vein virus. Pages 55-83 in: Rhizomania, E. Biancardi and T. Tamada, eds. Springer International Publishing, Cham, Switzerland.

Tamada, T., and Asher, M. J. C. 2016. The plasmodiophorid protist *Polymyxa betae*. Pages 135-153 in: Rhizomania, E. Biancardi and T. Tamada, eds. Springer International Publishing, Cham, Switzerland.

Tamada, T., Uchino, H., Kusume, T., Iketani-Saito, M., Chiba, S., Andika, I. B., and Kondo, H. 2021. Pathogenetic roles of beet necrotic yellow vein virus RNA5 in the exacerbation of symptoms and yield reduction, development of scab-like symptoms, and *Rz1*-resistance breaking in sugar beet. Plant Pathol. 70:219-232.

Tauzin, A. S., and Giardina, T. 2014. Sucrose and invertases, a part of the plant defense response to the biotic stresses. Front. Plant Sci. 5:293.

Vaïanopoulos, C., Legrève, A., Lorca, C., Moreau, V., Steyer, S., Maraite, H., and Bragard, C. 2006. Widespread occurrence of *Wheat spindle streak mosaic virus* in Belgium. Plant Dis. 90:723-728.

Vaïanopoulos, C., Legreve, A., Moreau, V., Steyer, S., Maraite, H., and Bragard, C. 2005. Occurrence of bymo- and furoviruses on wheat in Belgium. Parasitica 61:47-53.

van Loon, L. c., Rep, M., and Pieterse, C. m. j. 2006. Significance of inducible defense-related proteins in infected plants. Annu. Rev. Phytopathol. 44:135-162.

Wagh, S. G., Alam, M. M., Kobayashi, K., Yaeno, T., Yamaoka, N., Toriba, T., Hirano, H.-Y., and Nishiguchi, M. 2016. Analysis of rice RNA-dependent RNA polymerase 6 (OsRDR6) gene in response to viral, bacterial and fungal pathogens. J. Gen. Plant Pathol. 82:12-17.

Webb, K. M., Wintermantel, W. M., Kaur, N., Prenni, J. E., Broccardo, C. J., Wolfe, L. M., and Hladky, L. L. 2015. Differential abundance of proteins

in response to *Beet necrotic yellow vein* virus during compatible and incompatible interactions in sugar beet containing Rz1 or Rz2. Physiol. Mol. Plant Pathol. 91:96-105.

Webb, K. M., Wintermantel, W. M., Wolfe, L., Yao, L., Hladky, L. J., Broeckling, C. D., and Chaves, F. C. 2020. Metabolic disturbances in sugar beet (*Beta vulgaris*) during infection with *Beet necrotic yellow vein virus*. Physiol. Mol. Plant Pathol. 112:101520.

Wormit, A., and Usadel, B. 2018. The Multifaceted role of pectin methylesterase inhibitors (PMEIs). Int. J. Mol. Sci. 19:2878.

Yu, F., Wang, S., Zhang, W., Tang, J., Wang, H., Yu, L., Zhang, X., Fei, Z., and Li, J. 2019. Genome-wide identification of genes encoding putative secreted E3 ubiquitin ligases and functional characterization of PbRING1 in the biotrophic protist *Plasmodiophora brassicae*. Curr. Genet. 65: 1355-1365.

Zhang, X., Liu, Y., Fang, Z., Li, Z., Yang, L., Zhuang, M., Zhang, Y., and Lv, H. 2016. Comparative transcriptome analysis between broccoli (*Brassica oleracea* var. *italica*) and wild cabbage (*Brassica macrocarpa* Guss.) in response to *Plasmodiophora brassicae* during different infection stages. Front. Plant Sci. 7.

Zhou, M., Zhang, K., Sun, Z., Yan, M., Chen, C., Zhang, X., Tang, Y., and Wu, Y. 2017. LNK1 and LNK2 corepressors interact with the myb3 transcription factor in phenylpropanoid biosynthesis. Plant Physiol. 174: 1348-1358.

Ziegler-Graff, V. 2020. Molecular insights into host and vector manipulation by plant viruses. Viruses 12:263.

Ziegler-Graff, V., Bouzoubaa, S., Jupin, I., Guilley, H., Jonard, G., and Richards, K. 1988. Biologically active transcripts of beet necrotic yellow vein virus RNA-3 and RNA-4. J. Gen. Virol. 69:2347-2357.